Development 133, 1657-1671 (2006) doi:10.1242/dev.02341

Early, H^+-V-ATPase-dependent proton flux is necessary for consistent left-right patterning of non-mammalian vertebrates

Dany S. Adams[1], Kenneth R. Robinson[2], Takahiro Fukumoto[3,*], Shipeng Yuan[4], R. Craig Albertson[3], Pamela Yelick[3], Lindsay Kuo[3], Megan McSweeney[3] and Michael Levin[1,†]

Biased left-right asymmetry is a fascinating and medically important phenomenon. We provide molecular genetic and physiological characterization of a novel, conserved, early, biophysical event that is crucial for correct asymmetry: H^+ flux. A pharmacological screen implicated the H^+-pump H^+-V-ATPase in *Xenopus* asymmetry, where it acts upstream of early asymmetric markers. Immunohistochemistry revealed an actin-dependent asymmetry of H^+-V-ATPase subunits during the first three cleavages. H^+-flux across plasma membranes is also asymmetric at the four- and eight-cell stages, and this asymmetry requires H^+-V-ATPase activity. Abolishing the asymmetry in H^+ flux, using a dominant-negative subunit of the H^+-V-ATPase or an ectopic H^+ pump, randomized embryonic situs without causing any other defects. To understand the mechanism of action of H^+-V-ATPase, we isolated its two physiological functions, cytoplasmic pH and membrane voltage (V_{mem}) regulation. Varying either pH or V_{mem}, independently of direct manipulation of H^+-V-ATPase, caused disruptions of normal asymmetry, suggesting roles for both functions. V-ATPase inhibition also abolished the normal early localization of serotonin, functionally linking these two early asymmetry pathways. The involvement of H^+-V-ATPase in asymmetry is conserved to chick and zebrafish. Inhibition of the H^+-V-ATPase induces heterotaxia in both species; in chick, H^+-V-ATPase activity is upstream of *Shh*; in fish, it is upstream of Kupffer's vesicle and *Spaw* expression. Our data implicate H^+-V-ATPase activity in patterning the LR axis of vertebrates and reveal mechanisms upstream and downstream of its activity. We propose a pH- and V_{mem}-dependent model of the early physiology of LR patterning.

KEY WORDS: Left-right asymmetry, H^+-V-ATPase, V-ATPase, *Xenopus*, Chick, Zebrafish, Axial patterning, Cytoplasmic pH, Membrane voltage

INTRODUCTION

Consistent left-right (LR) asymmetries in the vertebrate body plan are of fundamental significance to both basic biology and medicine (Burn, 1991; Kosaki and Casey, 1998; Levin, 1999; Levin et al., 1996). Although the genetic cascades of secreted signals that occur on only one side of the embryo are being elucidated (Burdine and Schier, 2000; Whitman and Mercola, 2001), upstream mechanisms remain poorly understood (Levin, 2005; Yost, 2001). Recent findings shed light on the events which function upstream of asymmetric transcription (Bunney et al., 2003; Fukumoto et al., 2005b; Kramer et al., 2002; Levin and Mercola, 1998; Levin and Mercola, 1999; Tanaka et al., 2005), and it is now known that ion flux is involved in determining the laterality of several vertebrates and invertebrates (Duboc et al., 2005; Hibino et al., 2006; Levin et al., 2002; McGrath et al., 2003; Raya et al., 2004; Shimeld and Levin, 2006). To gain molecular insight into endogenous ion flows that control asymmetry, we performed a loss-of-function drug screen (Adams and Levin, 2006), implicating the H^+/K^+-ATPase (Levin et al., 2002). Here, we characterize another crucial component of early embryonic physiology: the H^+-V-ATPase.

The H^+-V-ATPase complex (see Fig. S1A in the supplementary material) or V-ATPase (Nishi, 2002), is found in the membranes of vacuoles where it acidifies the intravesicular environment (Inoue et al., 2003; Kawasaki-Nishi et al., 2003; Nishi, 2002). In many cell types, the H^+-V-ATPase is also present in the plasma membrane (Klein et al., 1997; Narbaitz et al., 1995; Nishi, 2002), where, by pumping protons out of the cell, it affects the pH of the cytoplasm and immediate extracellular environment (Brown and Breton, 2000; Kawasaki-Nishi et al., 2003; Scarborough, 2000). The H^+-V-ATPase is also strongly electrogenic (Harvey, 1992; Wieczorek, 1999).

Interestingly, besides the 'housekeeping' functions of the H^+-V-ATPase and other electrogenic proteins, their activity has been implicated in the control of cell proliferation, migration and differentiation (Levin, 2003a; Nuccitelli, 2003). One important example of morphogenesis relying upon precisely orchestrated cell behavior is the generation of consistent left-right asymmetry (Cooke, 2004; Levin, 2005), and a number of biophysical mechanisms based on bioelectricity and fluid movement have been implicated (Hamada et al., 2002; Levin, 2003c; Tabin and Vogan, 2003). Moreover, the conservation of early LR mechanisms is highly controversial (Burdine and Schier, 2000; Essner et al., 2002; Levin, 2003c). Although ion flux is crucial in early frog and chick embryos (Levin, 2005), ciliary motion has been implicated in rodents (McGrath and Brueckner, 2003; McGrath et al., 2003) and zebrafish (Amack and Yost, 2004; Essner et al., 2005; Kramer-Zucker et al., 2005). To understand how ion fluxes participate in asymmetry, it is

[1]The Forsyth Center for Regenerative and Developmental Biology, and Department of Developmental Biology, Harvard School of Dental Medicine, 140 The Fenway, Boston, MA 02115, USA. [2]Department of Biological Sciences, Purdue University, West Lafayette, IN 47906, USA. [3]Department of Cytokine Biology, The Forsyth Institute, 140 The Fenway, Boston, MA 02115, USA. [4]Cardiovascular Research Center, Massachusetts General Hospital, Harvard Medical School, Charlestown, MA 02129, USA.

*Present address: Weill Medical College, Cornell University, New York, NY 10021, USA
†Author for correspondence (e-mail: mlevin@forsyth.org)

Accepted 27 February 2006

necessary to characterize the endogenous behavior of the relevant pumps in embryos and to place their function in the context of known LR patterning mechanisms. Here, we explore the properties of H^+-V-ATPase function in several vertebrate embryos. Through endogenous localization of the H^+-V-ATPase and gain- and loss-of-function experiments in chick, frog and zebrafish, we identify the H^+-V-ATPase as a novel, conserved, obligate component of LR patterning upstream of asymmetric gene expression.

MATERIALS AND METHODS

Animal husbandry

Xenopus embryos were collected according to standard protocols (Sive et al., 2000) in 0.1× Modified Marc's Ringers (MMR) pH 7.8 + 0.1% Gentamicin. *Xenopus* embryos were staged according to Nieuwkoop and Faber (Nieuwkoop and Faber, 1967). Chick embryos from Charles River Laboratories, maintained at 38°C, were staged according to Hamburger and Hamilton (Hamburger and Hamilton, 1992). Zebrafish embryos (Westerfield, 1995) were maintained at 28.5°C in water containing 1 drop per gallon Methyl Blue.

Assaying organ situs

Xenopus embryos at stage 45 were analyzed for position (*situs*) of three organs: the heart, stomach and gallbladder (Levin and Mercola, 1998). Heterotaxia was defined as reversal in one or more organs (Fig. 1K,L). Only embryos with normal dorsoanterior development (DAI=5) and clear left- or right-sided organs were scored; percent heterotaxia was calculated as number heterotaxic divided by the number of scorable embryos, i.e. embryos normal in all other ways, with DAI=5. The proportion of unscorable embryos (number unscorable over total number of embryos), is reported as a measure of treatment toxicity, but has no influence on the heterotaxia score. The autofluorescence of gallbladder and pancreas was used to score situs in zebrafish embryos. A Pearson χ^2 (increased stringency) was used to compare absolute counts of heterotaxic embryos.

Pharmacological treatments

Xenopus embryos were incubated from 45 minutes post-fertilization to stage 6-7 in drugs (Fig. 1) at doses reported in Table 1. All of the reagents used were selected on the basis of high specificity for known electrogenic targets (Drose et al., 1993; Shen et al., 2003; Wheatly and Gao, 2004), and were titered to ensure that the DAI of the treated embryos was normal, thus avoiding confounding randomization caused by midline defects (Danos and Yost, 1996). Embryos were transferred to 0.1× MMR at stage 6-7and scored at stage 45. For all data shown, normal midline development and DAI were observed. For cytoskeleton disruption experiments (Fig. 3), embryos were treated with 50 nM nocodazole or with 0.7 μM latrunculin, in 0.1× MMR (Qiu et al., 2005).

To apply reagents to chick embryos with minimal disturbance, a small hole was made in each egg (prior to incubation), and 5 ml of light albumin removed. The experimental solution, consisting of pharmacological reagent (Table 1) in 5:1 light albumin and Pannett-Compton (Stern and Holland, 1993) was placed into the egg. Eggs were wrapped with Scotch tape, incubated at 37.5°C, then fixed in 4% paraformaldehyde.

Danio rerio embryos were incubated at 28.5°C in 1 μM lobatomide A16 or 250 nM concanamycin during stages indicated.

Self referencing ion selective probe measurements

For self referencing ion selective probe (SERIS) measurements of proton flux (Smith et al., 1999), healthy *Xenopus* embryos were cultured in 0.1× MMR at pH 7.0. H^+ flux measurements were made to the left and right, equidistant from the ventral midline, near the AV midline, slightly on the animal side, and approximately in the middle of the left-ventral quadrant and the right-ventral quadrant of the embryo. The displacement of the electrode was along a line that lay 45° from the normal to the surface of the embryo. This was true for both measuring positions. We calculate a correction factor of 105 for the presence of 0.5 mM HEPES buffer and have applied that factor to generate the absolute flux values reported in the Results section (Arif et al., 1995). The ratio of the fluxes across the ventral midline is unaffected by this correction. (Contact the authors for further details.)

Membrane voltage sensitive dye $DiBAC_4(3)$

Bis-(1,3-dibarbituric-acid)-trimethine-oxanol [$DiBAC_4(3)$, Molecular Probes] accumulates in proportion to membrane voltage; the more depolarized a cell, the greater the accumulation and fluorescence intensity of $DiBAC_4(3)$. Stock $DiBAC_4(3)$ (1 mg/ml in DMSO) was diluted 1:10 in distilled water, then 1:100 in 0.1× MMR (1.9 μM final). *Xenopus* embryos were soaked for 30 minutes, then imaged submerged in dye, using a Leica TCS SP2 Spectral Confocal Imaging System. The dye was excited at 488 nm and a 20 nm band of emission wavelengths centered at 515 was collected. On any given day, photomultiplier tube gain was kept constant to allow comparisons among images.

Expression analysis

Whole mount in situ hybridization (WISH) on *Xenopus* was performed using a standard protocol (Harland, 1991) using *XNr1* (Lohr et al., 1998; Lowe et al., 1996a), chick *Shh* (Levin et al., 1995) and chick *Nodal* (Levin et al., 1995) probes. WISH analysis was performed on zebrafish embryos as described (Albertson and Yelick, 2005). After staining, embryos were re-fixed in 4% paraformaldehyde, and dehydrated in 100% methanol overnight to remove background staining. Images were manipulated with Adobe Photoshop to increase clarity; data were neither added nor removed.

Immunocytochemistry was performed as described (Levin, 2004). Briefly, *Xenopus* embryos were fixed overnight at 4°C in MEMFA; chick embryos were fixed overnight in 4% PFA. Some embryos were embedded for 40 μm sectioning on a vibratome. Samples were blocked with 20% goat serum+0.2%BSA and incubated overnight at 4°C with primary antibody: anti-subunit A, 1:500 (Kawa et al., 2000); anti-myosin V, 1: 500 (Chemicon #AB5887), anti-RFX3, 1:500 (Bonnafe et al., 2004); anti-subunit F, 1:500 (Peng et al., 1996); anti-subunit c, 1:500 (against peptide DAGVRGTAQ, Invitrogen). After washing, samples were incubated overnight at 4°C with alkaline phosphatase-conjugated secondary antibodies. The chromogenic reaction was timed to optimize signal to noise ratio. Standard no-primary, no-secondary and peptide-adsorbed primary controls were used and resulted in no staining. Patterns reported for localization of V-ATPase subunits represent a consensus of data obtained from at least 15 embryos. Images were manipulated with Adobe Photoshop to increase clarity; data were neither added nor removed.

Microinjection of mRNAs

Xenopus embryos were injected with capped, synthetic mRNAs (Sive et al., 2000) into the animal hemisphere of one-cell embryos 45-90 minutes post-fertilization. NHE3 constructs were injected into the vegetal hemisphere within 60 minutes of fertilization. Zebrafish embryo microinjection was performed as described previously (Payne-Ferreira and Yelick, 2003). Results of injections are reported as: % of otherwise normal embryos that were heterotaxic; sample size (n); % of injected embryos that died or were abnormal after gastrulation and not scored; and χ^2 and P values comparing treated with controls.

RESULTS

Inhibition of H^+-V-ATPase specifically causes heterotaxia

To identify molecular candidates for electrogenic proteins involved in LR patterning, we performed a pharmacological loss-of-function screen (Fig. 1A-J, Table 1) (Adams and Levin, 2006; Fukumoto et al., 2005a; Fukumoto et al., 2005b; Levin et al., 2002; Mitchison, 1994). A panel of inhibitors targeting a wide variety of transporters (Fig. 1B-J), like many others reported previously (Levin et al., 2002), induced a very low incidence of laterality phenotypes, ruling out the corresponding targets from important roles in asymmetry and demonstrating the general stability of LR patterning. By contrast, inhibitors of the H^+-V-ATPase all induced strong heterotaxia (compare Fig. 1K with 1L) in the absence of changes in dorsoanterior character or general toxicity (Danos and Yost, 1995; Danos and Yost, 1996). For example, the potent and highly-specific V-ATPase blockers concanamycin (Huss et al., 2002) and bafilomycin (Bowman et al., 1988) induced heterotaxia in 35%

(*n*=100) and 36% (*n*=100) of the embryos respectively. Importantly, inhibition of the other two major classes of H^+ transporters, carbonic anhydrase (Fig. 1B) and the sodium-hydrogen exchanger (NHE, Fig. 1C), did not affect laterality. Specific and dose-dependent (Fig. 1M) randomization of LR asymmetry, induced by loss-of-function reagents targeting the H^+-V-ATPase, but not other H^+ pumps or a wide range of other ion transporters, implicate endogenous H^+-V-ATPase in the LR pathway in *Xenopus*.

To test unequivocally the requirement for H^+-V-ATPase activity using specific molecular reagents, we analyzed asymmetry in embryos injected with YCHE78 mRNA, which encodes a well-characterized dominant negative H^+-V-ATPase subunit E (Lu et al., 2002). Misexpression of this dominant-negative construct specifically induced 20% heterotaxia [(*n*=191), controls=4% (*n*=422), χ^2=40.6, $P \ll 0.001$]. By contrast, injection of mRNAs encoding the *Xenopus* H,K-ATPase α subunit (Mathews et al., 1995), or the dominant-negative Kir2.2 subunit (Zobel et al., 2003) did not cause heterotaxia (1% heterotaxia each, *n*=85,93 respectively). These data are consistent with the screen results, demonstrate that embryonic asymmetry is not generally labile with respect to microinjection per se (even when performed during cytoplasmic rotation), and strongly support the hypothesis that H^+-V-ATPase function is necessary for LR patterning.

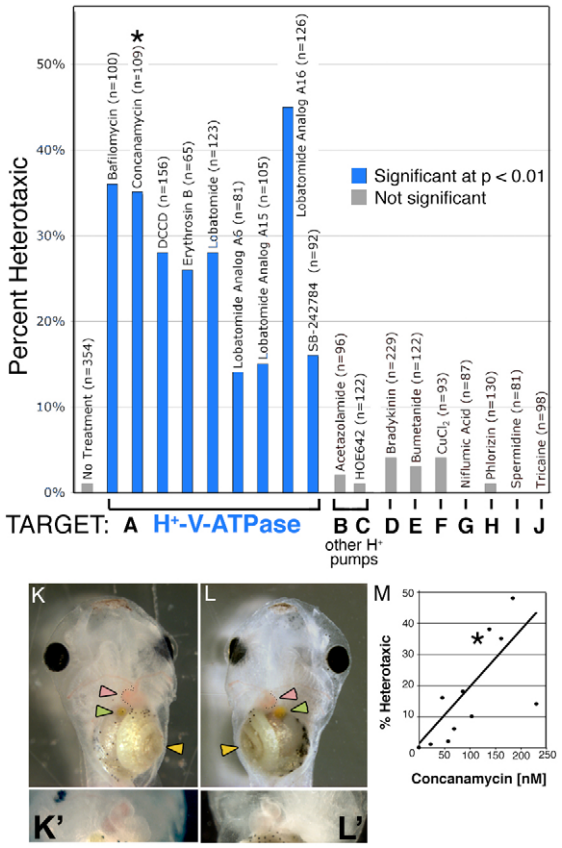

Fig. 1. Heterotaxia induced by H^+-V-ATPase inhibitors. *Xenopus* embryos were soaked in inhibitors of various ion transporters. The percent of embryos considered heterotaxic (defined as a reversal of at least one from the heart, gut or gall bladder) is calculated relative to the total number of embryos, most of which showed normal laterality. Inhibitors of H^+-V-ATPase (**A**) caused significant levels of heterotaxia, while inhibitors of other proton pumps (**B**,**C**) or of other transporters (**D-J**) had no effect on laterality. Inhibitor names and sample sizes are listed above the bars; targets and doses of drugs in B-J are listed in Table 1. Complete randomization of three organs would lead to a maximum heterotaxia rate of 87.5%, as, by chance, organ situs will appear to be wild type in 12.5% of embryos. (**K**) A wild-type embryo, ventral view, showing the normal arrangement of the gut (yellow arrowhead), heart apex (pink arrowhead) and gall bladder (green arrowhead). (K′) Higher magnification of normal heart. (**L**) A heterotaxic embryo (ventral view) showing reversal of all three organs, i.e. situs inversus. (L′) Close-up of reversed heart. Image contrast has been enhanced for clarity, and the loop of the heart has been outlined with black dots in K and L. Drugs used for this screen were titered to determine a dose that will cause heterotaxia without causing other morphological defects; (**M**) an example titration curve for concanamycin. The asterisk in M corresponds to the datum used in A (115 nM). There is a degree of variability among sensitivity of embryos obtained from different females; toxicity (defined as the percent of embryos dying post-gastrulation and/or developing with significant morphological defects) increases at larger concentrations, and there is only a narrow range of useful doses. The dose that is toxic to 50% of embryos (TD_{50}; corrected for control background lethality of 9%) was 234 nM.

H^+-V-ATPase inhibitors disrupt localization of normally left-sided transcripts

To determine the relationship between H^+-V-ATPase and the asymmetric gene cascade, we analyzed the expression of the earliest known asymmetric gene in *Xenopus*: *Nodal* (Hyatt et al., 1996). In embryos treated with the potent and specific heterotaxia-causing H^+-V-ATPase inhibitor concanamycin (Table 1), the situs of the left-sided marker *XNr1* (Fig. 2A) was effectively randomized (Fig. 2B-

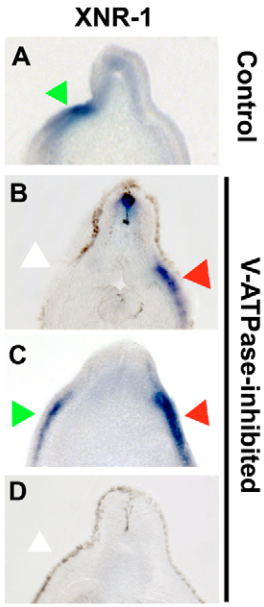

Fig. 2. In situ hybridization for *XNr1* in untreated and concanamycin-treated *Xenopus* embryos. Treatment of *Xenopus* embryos with the H^+-V-ATPase inhibitor concanamycin causes significant levels of heterotaxia that can be seen in the situs of organs at stage 45 (Fig. 1L), but disruptions of laterality can be detected much earlier by the expression patterns of normally left-sided markers. (A-D) Sectioned embryos processed for in situ hybridization with an *XNr1* antisense probe. In wild-type embryos, *XNr1* is restricted to the left (**A**); however, in inhibitor-treated embryos, its expression is randomized (**B-D**). Green arrows indicate normal position of staining; red arrows indicate ectopic expression domain; white arrows indicate lack of expression in normal region. Dorsal is upwards in all panels; left and right sides correspond to those of the reader.

Table 1. Pharmacological agents used in screen

Drug	Target	*Xenopus* dose	Reference
Acetazolamide	Carbonic anhydrase	0.1 mM	Layton and Hallesy (1965)
Bafilomycin A1	H^+-V-ATPase	0.2 mM	Bowman et al. (1988)
Bradykinin	Internal Ca^{2+} stores, NO	0.9 μM	Tokutomi et al. (1994)
Bumetanide	$Na^+/K^+/Cl^-$ co-transporter	0.9 mM	Landry et al. (1987)
Concanamycin	H^+-V-ATPase	6 nM (chick 250 nM)	Drose and Altendorf (1997)
$CuCl_2$	Tight junctions	0.01 μM	Ferruzza et al. (1999)
DCCD	H^+-V-ATPase	5 μM (chick 20 μM)	Finbow et al. (1993)
HOE642 (cariporide)	Na^+/H^+-ATPase	3 mM	Kondratev et al. (2005)
Lobatamide C	H^+-V-ATPase	0.4-0.8 μM	Shen et al. (2002)
Lobatamide C, analogue 6 (A6)	H^+-V-ATPase	0.15-0.3 μM	Shen et al. (2002)
Lobatamide C A15	H^+-V-ATPase	3 μM	Shen et al. (2002)
Lobatamide C A16	H^+-V-ATPase	0.6 μM (0.5 μM zebrafish)	Shen et al. (2002)
Palytoxin (PTX)	Na^+/K^+ ATPase	2 nM	Tosteson et al. (2003)
Niflumic acid	Ca^{2+}-activated Cl^- channels	3.5 μM	Myssina et al. (2004)
Phlorizin	Na^+/glucose co-transporter	0.1 mM	Kitlar et al. (1994)
SB-242784	H^+-V-ATPase	1 μM	Price et al. (2002)
Spermidine	NMDA receptor	0.6 mM	Biedermann et al. (1998)
Tributyl Tin (TBT)	OH^-/Cl^- exchanger	10 μM	Simchowitz et al. (1991)
Tricaine	Voltage-gated Na^+ channels	2 mM	Frazier and Narahashi (1975)

Drugs were stored as stock solutions then diluted to the above concentrations.

D), exhibiting aberrant sidedness of expression in 54% of the embryos (Table 2). We conclude that H^+-V-ATPase functions upstream of the asymmetric transcription of *Nodal* and feeds into the known asymmetric gene cascade.

H^+-V-ATPase subunits are asymmetrically localized in *Xenopus*

Because prior experiments and physiological data (below) indicated that the first cell cleavages are key to establishing ion flux-related asymmetries (Levin, 2003b; Levin et al., 2002), we focused our immunohistochemical analysis on the localization of H^+-V-ATPase subunits during the first few hours of development in *Xenopus*. In early embryos, most proteins are symmetrically localized with respect to the LR axis (Fig. 3A,B). Immunohistochemistry revealed that at the two-cell stage, H^+-V-ATPase subunits (Fig. 3D) exhibited 'fingers' extending up from a pool in the vegetal cytoplasm into the animal half. Such patterns are specific to a number of LR-relevant proteins but are not a general feature of all protein localization in the early frog embryo (Qiu et al., 2005) (Fig. 3A,B). In sections perpendicular to the AV axis at the two-cell stage, one cell was often more heavily stained (>80% of the embryos examined, Fig. 3E) (see Fig. S1I-K in the supplementary material), exhibiting both a cytoplasmic pool and localization at the cell cortex. At the four-cell stage, staining was still asymmetrical, and was on the right side in embryos that could be oriented by the cleavage furrows and pigmentation (Fig. 3F, see Fig. S1 in the supplementary material). Consistent with the proposed role of the H^+-V-ATPase in LR asymmetry, these electrogenic protein subunits are novel markers of LR asymmetry as early as the first two cleavages in *Xenopus*.

To probe upstream mechanisms (Qiu et al., 2005; Yost, 1991), we asked whether the asymmetric localization of H^+-V-ATPase required organized microtubules/microfilaments. Treatment of one-cell embryos with the actin depolymerizer latrunculin (Ayscough, 1998) caused apparently random localization of subunit A (Fig. 3G). By contrast, treatment with the microtubule disrupting agent nocodazole (De Brabander et al., 1986) had no obvious effect on the LR distribution of subunit A (Fig. 3H). Embryos treated with low levels of these specific cytoskeletal disruptors develop normally to later stages, but, consistent with these data, displayed randomized asymmetry (Qiu et al., 2005).

Early *Xenopus* embryos drive H^+-V-ATPase-dependent, asymmetric H^+ flux

In light of the loss-of-function and localization data, we asked whether the activity of H^+-V-ATPase (H^+ flux) might provide a consistently asymmetric physiological signal to the L and R sides of the body. Using a SERIS probe (Hotary et al., 1992; Smith et al., 1999; Smith and Trimarchi, 2001), we detected a large net efflux of protons from the cleavage furrow of the two-cell stage. This efflux averaged 12.7±22 pmole $cm^{-2}s^{-1}$ (n=5) at about the midpoint of cleavage. Importantly, we also found evidence for asymmetry of H^+-flux. As early as the four-cell stage, a distinct difference in proton efflux was detected across the ventral midline, with larger efflux occurring on the right side, consistent with the immunological localization of H^+-V-ATPase subunits on one side (Fig. 3F, see Fig. S1F,G,K in the supplementary material). In measurements on 15 embryos made between the four-cell stage and stage 6, the average proton efflux from the middle of the right ventral quadrant was 4.1±0.48 pmole $cm^{-2}s^{-1}$ and from the left ventral quadrant was 1.9±0.29 pmole $cm^{-2}s^{-1}$. The average ratio of the efflux from the right side to efflux from the left side was 2.3±0.3.

To confirm that the asymmetric efflux was due to asymmetric H^+-V-ATPase function, we compared H^+ efflux in control embryos with embryos treated with ion flux inhibitors. Neither the absolute net

Table 2. Effect of concanamycin on the sidedness of *XNR1* expression in *Xenopus*

***Nodal* expression**	**Left**		**Right**		**Bilateral**		**None**			
Treatment	*n*	%	*n*	%	*n*	%	*n*	%	χ^2	*P*
Control	34	94%	0	0%	0	0%	2	6%		
Concanamycin	144	46%	12	8%	27	19%	39	27%	24.0	⩽0.001

The laterality of expression of *XNR1* is significantly altered in frog embryos treated with the H^+-V-ATPase inhibitor concanamycin.

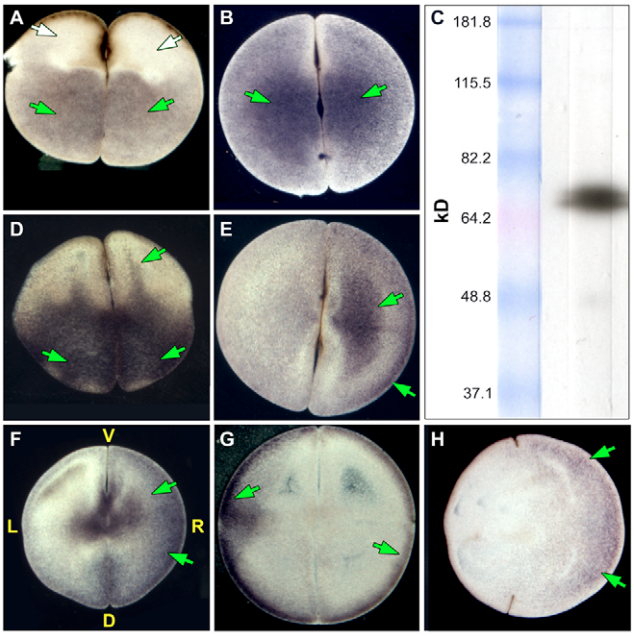

Fig. 3. Immunohistochemistry of H+-V-ATPase subunit A. Immunohistochemistry with an alkaline phosphatase conjugated secondary antibody for subunit A of the H+-V-ATPase. Embryos were oriented based on pigmentation and cleavage patterns – a technique that consistently reveals biased asymmetry among the L and R blastomeres with respect to a number of properties (Fukumoto et al., 2005b). Positive signals are blue to purple; LR orientation of embryos is only possible in four- and eight-cell embryos. (**A**) The molecular motor (Gross et al., 2002) myosin V (AV section i.e. parallel to AV axis) and (**B**) the ciliary protein (Bonnafe et al., 2004) RFX3 (flat section, i.e. perpendicular to the AV axis) are examples of symmetrically distributed proteins. (**C**) Western blot showing that the antibody detects a single band of approximately the right size (predicted: 69 kDa) for subunit A. Green and white arrows indicate positive and a lack of signal, respectively. (**D-H**) Immunostaining for subunit A. (D) Two-cell embryo, AV section, showing one common staining pattern: 'fingers' reaching animal-ward from the pool in the vegetal cytoplasm. Although this pattern is not exclusive to H+-V-ATPase subunits (Qiu et al., 2005), it is not found for many proteins (e.g. compare with A). (E) Flat section of a two-cell embryo showing another common staining pattern in which one blastomere is more heavily stained than its contralateral counterpart. (F) The asymmetry in staining seen in the flat sections is still visible at the four-cell stage when it is right-sided. (G) A flat section through a latrunculin-treated (actin depolymerized) embryo fixed at the four-cell stage, showing disruption of the normal pattern and loss of asymmetry in subunit A staining (compare with F). (H) A flat section through a nocodazole-treated (microtubules depolymerized) embryo showing that localization of subunit A can appear relatively unchanged by depolymerization of microtubules (compare with F).

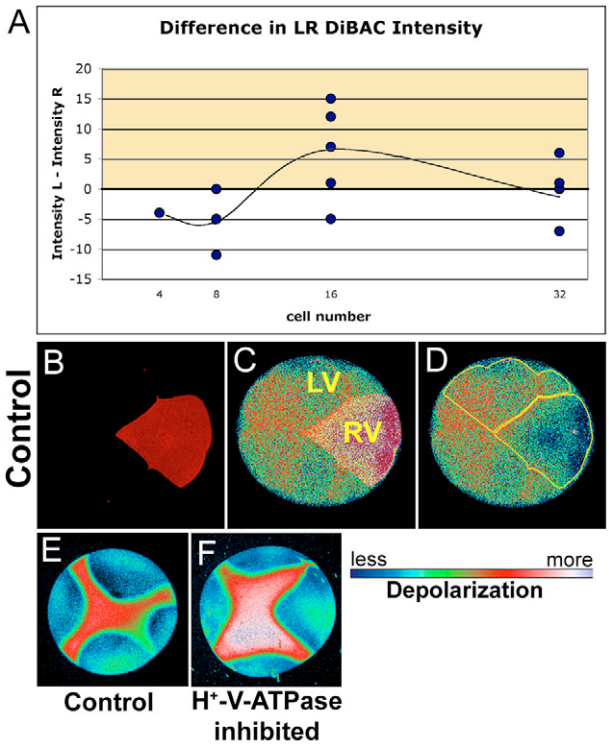

Fig. 4. DiBAC staining reveals the V_{mem} pattern of blastomere membranes under normal conditions and in H+-V-ATPase inhibitor. (**A**) Graph showing the difference in DiBAC intensity on the left versus the right ventral quadrants of the embryo. Positive values (yellow) indicate that the right side is hyperpolarized with respect to the left side; negative values indicate the inverse. At the 16-cell stage, the right side is hyperpolarized with respect to the left. (**B-D**) Example of DiBAC-stained 16-cell embryo; $DiBAC_4(3)$ intensity on the left was greater than on the right. Fluorescence intensity in C and D is pseudocolored; LUT shown below. (B) Alexa 647-10,000 M_r dextran (Molecular Probes) lineage labeled the right ventral quadrant. (C) Background-corrected maximum-projected series of confocal images of DiBAC fluorescence overlaid with lineage label to show location of left ventral (LV) and right ventral (RV) quadrants and the position of the ventral midline (between). (D) Regions of interest outlined in yellow. Mean pixel intensities in these two regions were used as measures of depolarization of cells on the two sides of the embryo. The difference between these two mean intensities was calculated to produce data in A. (**E**,**F**) $DiBAC_4(3)$ fluorescence from a four-cell embryo; (E) untreated and (F) treated with concanamycin. Consistent with the prediction that inhibiting the H+-V-ATPase will cause cells to depolarize (as H^+ builds up inside the membrane), concanamycin causes an increase in $DiBAC_4(3)$ fluorescence intensity visible here as the larger area of red and the area of white to lavender.

proton fluxes nor their right/left ratios were affected by the application of omeprazole (0.27 μM), an inhibitor of H^+/K^+-ATPase. However, the H+-V-ATPase inhibitor concanamycin (0.28 μM) reduced the proton efflux on the right side to about half of its original value and eliminated the LR asymmetry in the proton fluxes [ratio went from 2.1±0.2 to 1.1±0.05 (n=3), t=4.85, P<0.05]. Taken together, these data reveal the existence of consistent H^+ flux asymmetry in the four-cell embryo, and confirm that, as suggested by the localization data, the asymmetry in the flow of H^+ ions out of the early blastomeres is due specifically to differential H+-V-ATPase activity.

Because in many systems the H+-V-ATPase contributes significantly to the membrane voltage gradient V_{mem} (Gluck, 1992), we also used the reporting dye $DiBAC_4(3)$ to determine whether there is a consistent asymmetry to V_{mem} (Epps et al., 1994). Embryos marked with Alexa 647 dextran in the right ventral cell (RV) at the four-cell stage were monitored using $DiBAC_4(3)$ at 4-32 cells (Fig. 4). Although no pattern was obvious in 4-, 8- or 32-cell embryos, at 16 cells, we observed hyperpolarization of the RV quadrant, relative to the LV quadrant (Fig. 4A, yellow shading). An example of an embryo in which this difference is easily observed is shown in Fig. 4B-D. This pattern and its embryological timing are consistent with

the SERIS data, and with the hypothesis that higher net H^+ efflux on the right side at the four-cell stage results in a difference in membrane potential across the ventral midline by the 16-cell stage.

That this V_{mem} gradient is detectable in 16-cell embryos implies that H^+-flux-affecting reagents must be active by this stage in order to affect LR patterning. To test this prediction, we injected YCHE78 mRNA, the dominant-negative H^+-V-ATPase subunit E, into the LV or RV cell at the four-cell stage, which results in no detectable expression until the ~64-cell stage. This had no effect on organ situs [controls=0% (n=38, unscorable=4%), LV=0% (n=62, unscorable=10%), RV=1% (n=67, unscorable=12%)], χ^2=0.0, P=0.9), although co-injected GFP was expressed normally (DNS). Similarly, we injected YCHE78 DNA at the one-cell stage, which leads to protein expression only after zygotic transcription begins at mid-blastula transition. Co-injected β-gal DNA was expressed (and caused higher toxicity than mRNA injections), but injections had no effect on organ situs [β-gal DNA alone=0% (n=38, unscorable=65%), YCHE78 DNA=3% (n=29, unscorable=70%), χ^2=2.0, P=0.155]. These data are consistent with a dependence of LR asymmetry on very early, but not later, activity of H^+-V-ATPase.

Exogenous plasma-membrane H^+-pump activity causes heterotaxia

We next examined the effects of an excess, symmetrical H^+-flux across the plasma membrane on both sides of the midline. We induced ectopic H^+ flux by expressing a well-characterized single-subunit plasma-membrane H^+-pump, PMA1.2 (Masuda and Montero-Lomeli, 2000). Use of this construct also allowed us to address whether it is the balance of H^+ flux at the cell membrane that is important for LR asymmetry, as the H^+-V-ATPase is also known to occur in vacuoles, while PMA1.2 functions only in the cell membrane. Ubiquitous early misexpression of this H^+ pump at cell surfaces caused significant heterotaxia [PMA1.2=21% heterotaxic (n=135, unscorable=22%), untreated=2% (n=187, unscorable=3%), χ^2=28.3, $P\ll0.001$]. These data are consistent with the SERIS probe measurements and the importance of differential H^+ flux, and suggest that it is the flow of hydrogen ions across the cell, not vacuole, membrane that is important for LR asymmetry.

Manipulation of pH causes heterotaxia

To gain insight into the mechanisms by which the H^+-V-ATPase controls downstream events, we separately tested its two physiological roles – regulation of pH and membrane voltage – by experimentally altering these two parameters independently of direct manipulations of the H^+-V-ATPase. We first examined the effect of changing the pH of the external environment of the embryo by raising or lowering the pH of the medium during cleavage stages (Table 3). Although pH 7-11 had no effect on asymmetry, pH 5-6 caused a low level of LR patterning defects (6%, P=0.003), and pH 4 caused a significant level of heterotaxia (19%, $P\ll0.001$). This is consistent with inhibition of the activity of H^+-extruding pumps by high external proton concentrations. To alter embryonic pH without changing V_{mem}, we used the electroneutral OH^-/Cl^- exchanger tributyltin chloride (TBT, Table 1) to raise internal pH (Matsuya et al., 2000; Simchowitz et al., 1991). Treatment with 10 μM TBT from stages 1 to 13 caused heterotaxia in 17% of embryos [(n=151); untreated 1% (n=361); χ^2=44.7, $P\ll0.001$].

To study the effect of isolated changes in pH using greater molecular specificity, we overexpressed the electroneutral, plasma-membrane Na^+/H^+-exchanger NHE3 (Praetorius et al., 2000; Sabirov et al., 1999). Injection of this antiporter mRNA within 1 hour of fertilization caused heterotaxia [NHE3=16% (n=77, unscorable=32%), untreated=3% (n=114, unscorable=5%), χ^2=8.9, P=0.003]. This confirms the importance of pH for LR asymmetry, and, similar to the PMA1.2 data, indicates that the relevant H^+ flux occurs at the cell membrane, not in vesicles. Interestingly, NHE3 was active in causing heterotaxia only when injected in the vegetal hemisphere and when injected within 60 minutes of fertilization; later injections had no effect. Assuming that NHE3 mRNA is translated ~1.5 hours after injection (based on detection of β-gal/GFP translation), the temporal window during which NHE3 can cause heterotaxia ends by 2.0 to 2.5 hours post-fertilization at 18°C. Consistent with expression data, the asymmetric membrane voltages at 16-cell stage, and the lack of effect on asymmetry of late YCHE78 injection or DNA injection, we conclude that the LR-relevant gradients in cell membrane H^+ flux occur during the first cleavages, and that normal asymmetric pH at the cell membrane is crucial for LR patterning.

Table 3. Effect of medium pH on laterality of *Xenopus* embryos

pH of medium	Sample size (n)	Heterotaxic	χ^2	P
7.8 (control)	334	1%	–	–
4	129	19%	46.6	⩽0.001
5	108	6%	7.3	0.007
6	122	6%	6.0	0.014
7	110	0%	0.3	0.568
8	152	0%	0.7	0.416
9	106	0%	0.3	0.586
10	101	1%	0.1	0.718
11	95	4%	2.2	0.137

Embryos were kept in 0.1× MMR at different pHs (column 1) from the one-cell stage to stage 12-13, then scored for organ position at stage 45. At pH 7 or above, embryos were no different from controls. At pH 6 and 5, the incidence of heterotaxia increased to low but significant levels. At pH 4, 19% of embryos were heterotaxic.

Manipulation of V_{mem} causes heterotaxia

The H^+-V-ATPase is electrogenic (Gluck, 1992; Harvey and Wieczorek, 1997) and can therefore significantly contribute to the steady-state V_{mem}. We confirmed this in *Xenopus* blastomeres by imaging V_{mem} in vivo in control and concanamycin-treated embryos. As predicted, inhibition of H^+-V-ATPase depolarizes V_{mem} (Fig. 4E,F). We conclude that H^+-V-ATPase activity is necessary for the normal pattern of V_{mem} in *Xenopus*.

To address the role of V_{mem} in the absence of pH changes, we altered V_{mem} directly by incubating embryos in the Na^+/K^+ inhibitor palytoxin (PTX), which converts the Na^+/K^+-ATPase into a non-specific ion channel, thus dissipating the voltage gradient and depolarizing cells (Hilgemann, 2003; Tosteson et al., 1997; Tosteson et al., 2003). PTX treatment (2 nM) of embryos from stage 1-6 caused heterotaxia in the absence of DAI change or other defects in 20% of surviving treated embryos [(n=60, unscorable=84%), untreated=2% (n=58, unscorable=3%), χ^2=8.3, P=0.004]. We conclude that normal V_{mem}, or patterned differences in V_{mem}, are necessary for normal asymmetry.

H^+-V-ATPase is present in early chick and zebrafish embryos

To explore the evolutionary conservation of an H^+-V-ATPase-dependent LR-patterning mechanism, we characterized the expression pattern of H^+-V-ATPase subunits in chick and zebrafish. In situ hybridization analysis of subunits A, c, and F (Fig. 5A-D), and immunocytochemistry for subunits F and c (Fig. 5E-H) indicated that the H^+-V-ATPase is expressed in the primitive streak

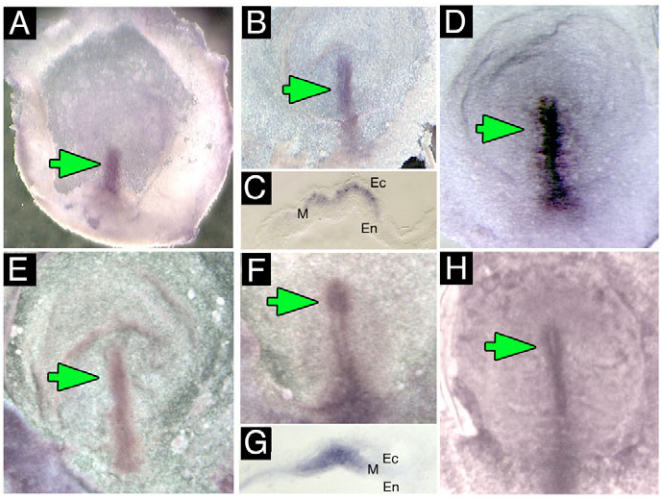

Fig. 5. Expression of H+-V-ATPase subunits in early chick embryos. (**A-D**) Whole-mount in situ hybridization for H+-V-ATPase subunits; green arrows indicate normal location of staining. (A) Whole-mount in situ hybridization for subunit A in stage two chick embryos. Staining is in the primitive streak. (B) Whole-mount in situ hybridization for subunit A at stage 3 showing staining along the length and through to the tip of the primitive streak. (C) Section through the primitive streak of a stage 3 embryo reveals expression in the mesoderm. (D) Stage 4⁻ embryo probed for subunit F, which, like subunits A and B, is found in the primitive streak, extending through Hensen's node. (**E-H**) Immunostaining for H+-V-ATPase subunits. (E) Stage 2+ chick embryo reveals subunit B along the length of the primitive streak. (F) In stage 3 chicks, staining for subunit B is in the streak and the node. (G) Cross-section through the streak of a stage 3 embryo showing subunit a staining in the mesoderm (M); Ec, ectoderm; En, endoderm. (H) Subunit B staining in a stage 4 chick. The streak and node are both positive.

of chick embryos at stages 2-4, and in the node at stage 4 – the time-period in which chick LR sidedness is determined by depolarization in the streak (Levin et al., 2002). Zebrafish embryos (Fig. 7A-F) showed immunohistochemical staining for subunit c in two- to eight-cell stage embryos. By the 32-cell stage, staining appeared stronger in the marginal cells. Early in epiboly, staining was even in all cells, and subunit c was detected surrounding some yolk syncytial nuclei. Staining was apparent in all cells at epiboly.

Cellular pH control and *Shh*/*Nodal* expression in chicks require H+-V-ATPase function

First, to confirm that H+-V-ATPase is upstream of LR patterning events in chick, we examined the effect of H+-V-ATPase inhibition on the expression of the early left-sided marker, and correlate of heart looping, sonic hedgehog (Levin et al., 1995). Inhibition of H+-V-ATPase by concanamycin (Woo et al., 1996) or DCCD (Finbow et al., 1993) specifically randomized the localization of *Shh* and *Nodal* (Fig. 6A-D) Concanamycin induced aberrant sidedness of *Shh* expression in 67%, and *Nodal* in 24%, of embryos (Table 4). Thus, as in *Xenopus*, H+-V-ATPase is upstream of the known asymmetric gene cascade, and is required for normal *Nodal* expression and therefore normal LR patterning in chick.

Next, we assayed whether the pattern of cellular pH in the early chick blastoderm requires H+-V-ATPase activity. Using the pH reporting dye SNARF-1-AM (Buckler and Vaughan-Jones, 1990; Morley et al., 1996), we found that in control embryos, area pellucida cells maintain higher intracellular pH than primitive streak

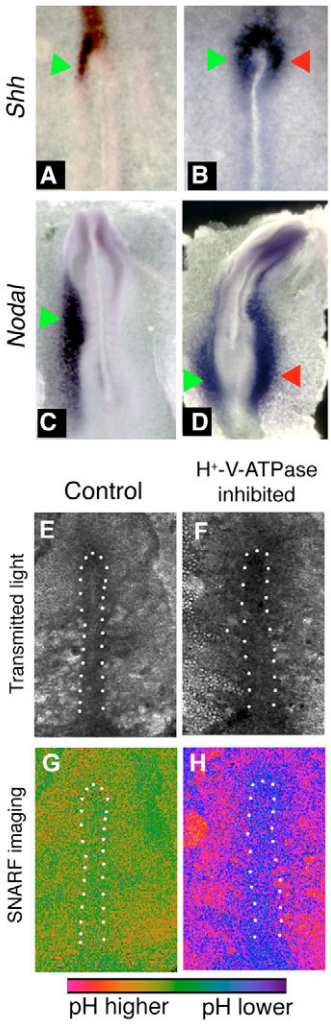

Fig. 6. In situ hybridization for sonic hedgehog and *Nodal*, and pH imaging, in concanamycin-treated chick embryos. Embryos exposed to vehicle alone exhibited the normal left-sided expression of *Shh* (**A**) and *Nodal* (**C**). When exposed to the H+-V-ATPase inhibitor concanamycin during early streak stages, the left-sided expression becomes destabilized (see Table 4). Examples include bilateral expression of *Shh* (**B**) or *Nodal* (**D**). Culture of chick embryos can lead to bending of the AP axis such as that of embryo in D. In our experiments, about 15% of both control and treated embryos show this bend. Green arrows indicate normal position of staining; red arrows indicate ectopic expression domain. (**E-H**) Embryos treated with the pH indicator cSNARF-5F. Anterior is upwards and left is leftwards in all images. White dots indicate the approximate boundaries of the primitive streak. (E,F) Transmitted light images of two embryos. (G) Pseudocolored image of ratiometric data representing pH, shown in control embryo E. In most images, pH of the primitive streak is somewhat lower than pH of the surrounding area pellucida (AP) cells; the degree of contrast varies and is somewhat low in the image shown. (H) In concanamycin-treated embryos, the primitive streak cells (which stain positively for H+-V-ATPase subunits; see Fig. 5E-H) are at a lower pH than control cells (purple compared to green; embryo F). The AP, by contrast, is at a higher pH than controls. The difference between pH of the primitive streak and pH of the AP is much more pronounced in concanamycin-treated embryos.

cells (Fig. 6G,H). And, as predicted by the expression of the H+-V-ATPase in the primitive streak, the H+-V-ATPase inhibitor concanamycin lowers the pH of streak cells.

Table 4. Effect of concanamycin on the sidedness of the expression of *Shh* and *Nodal* left-side markers in chick

	Expression	Left		Right		Bilateral		None			
Gene	Treatment	*n*	%	*n*	%	*n*	%	*n*	%	χ^2	*P*
Shh	Control	17	100%	0	0%	0	0%	0	0%		
	Concanamycin	15	33%	3	7%	17	38%	10	22%	19.370	≪0.001
Nodal	Control	25	100%	0	0%	0	0%	0	0%		
	Concanamycin	43	77%	0	0%	6	11%	7	13%	5.297	0.001

The laterality of expression of *Shh* and *Nodal* is significantly altered in chick embryos treated with the H^+-V-ATPase inhibitors concanamycin or DCCD.

The concanamycin-induced decrease in pH in the primitive streak is consistent with H^+-V-ATPase being the main regulator of pH in these cells. More difficult to interpret is the change in pH of the AP. Neither in situ hybridization nor immunohistochemistry reveals H^+-V-ATPase subunit expression in the AP; thus, it was surprising that the highly specific H^+-V-ATPase inhibitor concanamycin affected the AP. One interpretation is that while our imaging studies have only revealed the location of plasma-membrane associated H^+-V-ATPase, concanamycin treatment also affects the intracellular vesicle-associated H^+-V-ATPase, and it is that which affects pH in AP cells.

H^+-V-ATPase function is upstream of Kupffer's vesicle function

To further examine evolutionary conservation of the V-ATPase, we disrupted its function in *Danio rerio* embryos. As in *Xenopus*, microinjection into fertilized zebrafish eggs of mRNAs encoding a dominant-negative subunit E mRNA caused a high level of heterotaxic organ situs [YCHE78=36% (*n*=42, unscorable=0%), untreated=5% (*n*=96, unscorable=4%), χ^2=19.5, *P*≪0.001; Fig. 7G-I]. Injections of mRNA for NHE3, to alter cytoplasmic pH only, caused 34% heterotaxia, [(*n*=99, unscorable=6%), untreated=5% (*n*=94, unscorable=1%), χ^2=23.4, *P*≪0.001]. Expression of PMA1.2, to exogenously increase cell membrane H^+ flux, caused 29% heterotaxia, [(*n*=52, unscorable=9%), untreated=5% (*n*=96, unscorable=4%), χ^2=14.2, *P*≪0.001]. Taken together, these data support the hypothesis that specific levels and/or distributions of H^+-V-ATPase-dependant H^+ transport activity at the plasma membrane are necessary for correct LR asymmetry in zebrafish embryos.

Although molecular loss- and gain-of-function experiments demonstrate the importance of H^+-V-ATPase-dependent H^+ flux, they do not reveal the endogenous timing of H^+-V-ATPase function in fish. This is important as no mechanisms upstream of Kupffer's

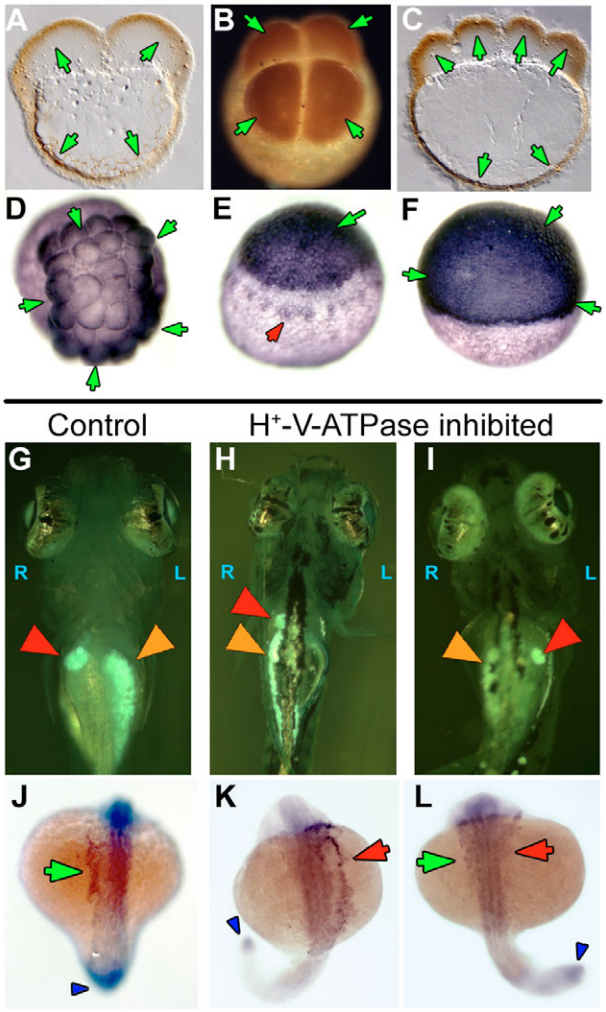

Fig. 7. H^+-V-ATPase subunits and heterotaxia in zebrafish. (**A-F**) Immunohistochemistry for H^+-V-ATPase subunits in zebrafish embryos: (A) subunit F in a two-cell embryo; (B) subunit c in a four-cell embryo; (C) subunit F in an eight-cell embryo. Brown (HRP-conjugated secondary) indicates a positive signal. At these stages, the cortical cytoplasm of all cells is positive for these two subunits, as is the cortical cytoplasm of the yolk cell. (D) Thirty-two-cell zebrafish embryo stained for subunit c. Staining (blue, AP-conjugated secondary) is heaviest in the marginal cells of this stage, but present in all cells. (E) Early in epiboly, subunit c staining is dark in the cells of the spreading blastoderm. In addition, staining is visible around a ring of yolk syncitial nuclei, probably representing vesicle staining (red arrowhead). (F) Once epiboly is more than 50% complete, immunohistochemistry for subunit c shows an even and heavy distribution in all the cells of the blastoderm. The antibodies used in this figure did not work in western blots on chick and fish extracts. (**G-I**) Heterotaxia in zebrafish larvae. Tricaine-anaesthetized 5- to 6-day larvae were examined on a Zeiss StemiSV11 dissecting microscope under 488/40 nm illumination, using a 510 nm barrier filter. An embryo was considered heterotaxic if either pancreas (orange arrowheads), gall bladder (red arrowheads) or both organs were on the side opposite normal. (G) Normal position of gall bladder (right) and pancreas (left). (H) Heterotaxia involving the pancreas. (I) Heterotaxia involving both organs. When scoring two organs, the top heterotaxia rate is 75% as, by chance, organ situs will appear to be wild type in 25% of fully randomized embryos. (**J-L**) Whole-mount in situ hybridization for the nodal-related gene southpaw (*Spaw*), which is expressed in the left lateral plate mesoderm (LPM) and tailbud of wild-type embryos from approximately 15-somite to 22-somite stage. (J) Untreated embryos at 20-22-somite stages showed wild-type *Spaw* expression in the left LPM (green arrow). *Spaw* expression in the tail bud (an internal positive control for the specificity of the treatment on *Spaw* asymmetry) is indicated by a blue arrowhead. Similarly staged embryos treated early with the H^+-V-ATPase inhibitor lobatomide A16 exhibited reversed (K, red arrow) and bilateral (L, green and red arrows) *Spaw* expression (Long et al., 2003). See Table 5 for statistical analysis.

Table 5. Effect of H+-V-ATPase inhibitors on the sidedness of the expression of *Spaw*, a left-side marker in zebrafish

	Expression	Left		Right		Bilateral		None			
Gene	Treatment	*n*	%	*n*	%	*n*	%	*n*	%	χ^2	*P*
Spaw	Control	25	93%	1	4%	1	4%	0	0%		
	A16	17	45%	9	24%	12	32%	0	0%	13.787	≪0.001
	Control	22	92%	1	4%	1	4%	0	0%		
	Concanamycin	11	42%	9	35%	6	23%	0	0%	11.439	≪0.001

The laterality *Spaw* expression is significantly altered in zebrafish larvae treated with the H+-V-ATPase inhibitors lobatomide A16 or concanamycin.

vesicle (KV) (Amack and Yost, 2004) have yet been discovered in zebrafish asymmetry. To determine whether the H+-V-ATPase is involved early, as in *Xenopus*, or later, at stages when cilia might be involved (Essner et al., 2005), we used the specific H+-V-ATPase inhibitors lobatamide A16 (Shen et al., 2002) and concanamycin (Huss et al., 2002). As in *Xenopus* and chicks, initiation of H+-V-ATPase loss-of-function between fertilization and the two-cell stage causes significant heterotaxia [A16=30% (*n*=119), untreated=2% (*n*=138), χ^2=37.0, *P*≪0.001; concanamycin=30% (*n*=87), χ^2=34.1, *P*≪0.001, phenotypes same as shown in Fig. 7G-I]. By contrast, exposure to lobatamide A16 beginning at three somites (just prior to the formation of KV) did not result in a significant level of heterotaxia [A16=5% (*n*=56), χ^2=0.0, *P*=0.85]. Thus, in zebrafish embryos, H+-V-ATPase-dependent H+ flux is important prior to the three-somite stage, i.e. prior to KV formation, and is the earliest known step in LR patterning in zebrafish.

Consistently, treatment with the H+-V-ATPase blocker lobatamide A16 resulted in 55% right/bilateral expression of the asymmetric (left-sided) marker *Southpaw* (Long et al., 2003) [Fig. 7J-L (*n*=38), untreated=7% (*n*=27), χ^2=13.8, *P*≪0.001). Similar results were obtained using concanamycin [treated=58% (*n*=26), untreated=8% (*n*=24), χ^2=11.4, *P*=0.001; Table 5), demonstrating that H+-V-ATPase activity is upstream of the earliest known asymmetric marker in zebrafish.

The movement of cilia in KV of fish is important for normal asymmetry (Essner et al., 2005; Kramer-Zucker et al., 2005) and we analyzed the interaction of H+-V-ATPase function with the cilia pathway. Although H+-V-ATPase was not detected on the surface of KV cilia (Fig. 8A), we found that treatment of zebrafish embryos with the H+-V-ATPase inhibitors lobatamide A16 or concanamycin caused the KV cilia to appear short and/or greatly reduced in number [Fig. 8B,C; untreated=15% (*n*=41); A16=41% (*n*=39), χ^2=5.7, *P*=0.017; concanamycin=52% (*n*=27), χ^2=9.1, *P*=0.002]. We conclude that H+-V-ATPase activity is upstream of the LR signaling events that are dependent on normal KV cilia.

H+-V-ATPase function is required for normal serotonin localization

Finally, we linked the H+-V-ATPase to another known early LR patterning mechanism: serotonin, which plays an important early role in frog and chick embryos (Fukumoto et al., 2005a; Fukumoto et al., 2005b). In *Xenopus*, serotonin is initially present in all blastomeres but is localized to one blastomere by the 16/32 cell stages (Fig. 8D,F). By contrast, embryos exposed to the specific H+-V-ATPase blocker concanamycin exhibited an almost complete absence of serotonin content (Fig. 8E,G, *n*=17). We conclude that H+-V-ATPase activity is required for the maintenance of serotonin within early blastomeres and its localization to one specific cell, placing the activity of this pump upstream of serotonin signaling in the LR pathway.

DISCUSSION

H+-V-ATPase activity is required for correct LR asymmetry

The strong and specific randomization (Fig. 1A) of the heart and viscera by H+-V-ATPase blockers (which function by different mechanisms) but not by inhibition of other ion channels/pumps, clearly implicated the H+-V-ATPase as a promising novel candidate required for LR asymmetry. Although the H+-V-ATPase has housekeeping roles (Nishi, 2002), we were able to use inhibitors at

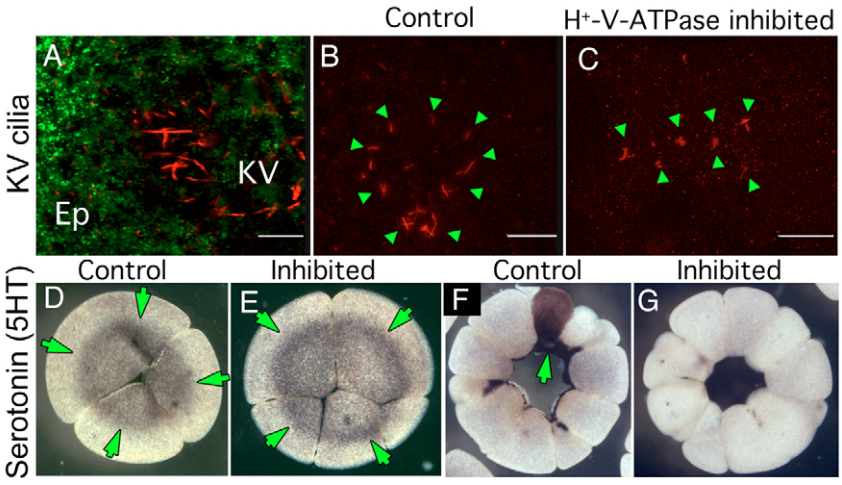

Fig. 8. Effect of early H+-V-ATPase inhibition on Kupffer's vesicle cilia and localization of serotonin. (**A**) Oblique confocal section through an 8-somite zebrafish larva doubly immunostained for H+-V-ATPase subunit A (green) and acetylated tubulin (red). Although subunit A is obvious in cells of the overlying epithelium (Ep), no H+-V-ATPase subunits are associated with KV cilia. (**B**,**C**) IHC for acetylated tubulin reveals the structure of KV cilia (green arrowheads) in five- to seven-somite stage zebrafish embryos. (B) Untreated embryo showing the characteristic circular field of long straight cilia, (C) KV cilia of five- to seven-somite embryos, soaked in H+-V-ATPase inhibitors from the one-cell to shield stage, are often reduced in number, altered in distribution or appear foreshortened relative to controls. (**D**,**E**) Immunohistochemistry for serotonin (5-HT, green arrows) in four-cell *Xenopus* embryos using an antibody previously shown to be specific for 5-HT (Levin, 2004); (D) untreated, (E) incubated in concanamycin from the one-cell stage. At this stage, there is no effect of H+-V-ATPase inhibition on 5HT localization (green arrows) or level. (**F**,**G**) Immunohistochemistry for 5HT in 32-cell *Xenopus* embryos; (F) normal pattern of 5HT staining in one cell in an untreated embryo (green arrows); (G) 5HT is absent from the H+-V-ATPase inhibited embryo.

doses that affected LR asymmetry strongly while permitting otherwise normal development (Fig. 1L). Use of specific blockers likewise implicated the H^+-V-ATPase in the control of laterality in the chick and zebrafish (Figs 6, 7), revealing this versatile pump as the first endogenous asymmetry mechanism conserved in three vertebrates.

Crucially, to unequivocally confirm the requirement for the H^+-V-ATPase, we augmented drug experiments with specific constructs targeting the H^+-V-ATPase. Misexpression of the dominant-negative E subunit (Lu et al., 2002) in *Xenopus* and in zebrafish embryos causes randomization, confirming the requirement for H^+-V-ATPase for correct asymmetry. Though changing V_{mem} and pH by overexpression can randomize, only the V-ATPase is implicated endogenously in setting LR-relevant values of these physiological parameters, as specific inhibitors of the Na^+/K^+-ATPase (Levin et al., 2002) and other H^+ pumps (Fig. 1) do not cause heterotaxia. Because genetic loss of H^+-V-ATPase activity in mice causes early embryonic lethality (Sun-Wada et al., 2000), the connection between this mechanism and rodent nodal cilia is unknown. Intriguingly, however, inhibition of carbonic anhydrase causes a LR-relevant phenotype in mice (Brown et al., 1989) but not in *Xenopus* (Fig. 1B). Perhaps control of pH is the common denominator, while the mechanism of that control has diverged among phyla.

Asymmetry-relevant H^+-V-ATPase activity takes place early in embryogenesis

Loss-of-function of the H^+-V-ATPase in chick randomizes the early left-sided marker *Shh* (Fig. 6B). This implies that, as in *Xenopus*, in chicks the H^+-V-ATPase functions upstream of early asymmetric gene expression. Future efforts to model physiological events that are integrated at the node must take into account not only electroneutral H^+/K^+ exchange (Levin et al., 2002) and Ca^{2+} flux (Raya and Belmonte, 2004; Raya et al., 2004), but also pH and/or V_{mem} regulation by H^+-V-ATPase. In zebrafish embryos, randomization of visceral situs and of *Spaw* localization, and disruption of KV cilia, was caused by H^+-V-ATPase inhibition prior to somite formation, suggesting that H^+-V-ATPase is the earliest-known component of the LR pathway in fish embryos, and acts prior to, and upstream of, events in KV (Amack and Yost, 2004; Essner et al., 2005; Kramer-Zucker et al., 2005). This implies that ciliary action, at least in zebrafish, is an important, but not initial, step in LR patterning (Okada et al., 2005). Interestingly, although inhibition of H^+-V-ATPase affects KV cilia, inhibition of the LR-crucial H^+/K^+-ATPase does not (Kawakami et al., 2005), suggesting that the zebrafish relies on ion fluxes at more than one LR signaling step. Further study of the interaction between early ion flux and ciliary events in fish will be interesting, as this is the first species in which both membrane voltage/pH and ciliary action are involved.

As with the H^+/K^+-ATPase (Levin et al., 2002), the earliest asymmetries of H^+-V-ATPase were observed in *Xenopus*. Maternal H^+-V-ATPase proteins are present, and asymmetries in their localization, and in directly detectable H^+-V-ATPase-dependent H^+ flow, exist by the 2nd cleavage in some percent of embryos. Alteration of H^+-V-ATPase function randomized *Nodal* (Fig. 2), the earliest available *Xenopus* asymmetric marker (Lowe et al., 1996b), placing it upstream of the conserved cascade in frog. Global upregulation of H^+ flux using the exogenous NHE3 pump did not affect laterality when injection of the construct took place later than 1.5 hours post-fertilization. Likewise, later inhibition of H^+-V-ATPase, caused by injections of YCHE78 mRNA at the four-cell stage or injections of YCHE78 DNA, also had no effect on organ situs. DiBAC fluorescence, used to reveal differences in membrane potential show biased asymmetry at the 16-cell stage; it is important to note, however, that because of the magnitude of, and the variations in cell volume, DiBAC is probably not accurate at earlier stages. Thus, a consistent asymmetry in V_{mem} may be present earlier. Localization of H^+-V-ATPase subunits to the right ventral cell of four-cell embryos, vibrating probe data showing enhanced H^+-efflux from the right ventral cells of four- and eight-cell embryos, and DiBAC fluorescence showing the right ventral quadrant to be hyperpolarized at the 16-cell stage, all support a role for H^+-V-ATPase activity during the first few hours of frog development.

Endogenous expression and mechanisms upstream of H^+-V-ATPase asymmetries

Consistent with the loss-of-function results, expression analysis revealed that H^+-V-ATPase subunits are present in chick from streak initiation (Fig. 5A) and in zebrafish (Fig. 7A) from the first cleavage. We detected no consistent asymmetries of expression in either species, similar to the situation for H^+/K^+-ATPase (Levin et al., 2002). It is likely that protein-level regulators remain to be discovered, the asymmetries of which confer functional asymmetries on the activity of pumps that are present symmetrically.

Asymmetrical localization of maternal components of the H^+-V-ATPase was observed after the first cleavage in *Xenopus* (Fig. 3). Although the plane of first cleavage can be experimentally repositioned (Black and Vincent, 1988; Danilchik and Black, 1988), in normal embryos the cleavage furrow usually corresponds to the future midline of the embryo (Klein, 1987; Masho, 1990), and injection of one cell at the two-cell stage is routinely used to target half the embryo, allowing the contralateral half to serve as an internal control (Harvey and Melton, 1988; Vize et al., 1991; Warner et al., 1984). Thus, consistent with the timing data, this early asymmetry of localization is likely to be key to the involvement of the H^+-V-ATPase in LR patterning of the whole embryo.

In light of early work from the Yost laboratory suggesting that organization of the cytoskeleton prior to 1st cleavage is required for LR asymmetry in *Xenopus* (Yost, 1991), the accepted role of the cytoskeleton and motor proteins in the localization of subcellular components, and data implicating dyneins and kinesins (Nonaka et al., 1998; Supp et al., 1997), we examined the interaction of the cytoskeleton with the H^+-V-ATPase (Fig. 3F-H). Consistent with earlier observations linking embryo-wide asymmetry with subcellular organization (Bunney et al., 2003), and recent work showing that H^+-V-ATPase subunits interact directly with the actin cytoskeleton (Chen et al., 2004; Lee et al., 1999; Vitavska et al., 2003), we found that the asymmetric targeting of the H^+-V-ATPase is dependent on actin, but not microtubule, organization. We propose that some as yet uncharacterized aspect of subcellular targeting (Al-Awqati, 1996; Brown, et al., 1992) [perhaps oriented by a nucleation center which fits the role of Wolpert and Brown's 'F-molecule' (Brown and Wolpert, 1990)] is upstream of the H^+-V-ATPase in the LR pathway. The ability of very early latrunculin exposure to randomize LR asymmetry in embryos (Qiu et al., 2005) is consistent with the observed effects on localization, linking cytoskeletal organization with large-scale asymmetry. We are currently investigating cytoskeletal processes that assure asymmetric localization of ion pumps.

The physiology of H^+-V-ATPase function and H^+ efflux in asymmetry

As the H^+-V-ATPase normally energizes both vesicle and plasma membranes, it is important to consider which of these roles controls asymmetry. The SERIS measurements show that significant

asymmetric flux can be detected at the cell surface. Moreover, equalizing asymmetries of H^+ flux at the cell membrane, by global overexpression of gain-of-function constructs (NHE3 and PMA1.2) that are known to induce H^+ flux specifically from cell surfaces, alters asymmetry in both frog and zebrafish. Thus, efflux of H^+ ions from the cell surface is one crucial function of the H^+-V-ATPase complex. However, it cannot conclusively be ruled out that subcellular-compartment pH may be important, and vesicular transport at the node could be such a locus (Tanaka et al., 2005).

What aspect of H^+-V-ATPase activity is required for asymmetry? We distinguished between the two H^+-V-ATPase functions, pH and V_{mem} regulation. Manipulating pH directly in different ways, using changes in medium pH, TBT and ectopic overexpression of the H^+ pump NHE3 in the blastomere plasma membrane, all disrupted asymmetry, consistent with our conclusion that control of pH by H^+-V-ATPase is important. In particular, as the NHE3 pump is electroneutral, its ability to randomize suggests that the normal pattern of pH in blastomeres is required for normal LR asymmetry. Because H^+-V-ATPase is also electrogenic, we explored the effect on LR asymmetry of changing V_{mem} independently of changes to the H^+-V-ATPase, using palytoxin, which directly abolishes V_{mem}. Like manipulation of H^+-V-ATPase activity and of pH, loss of V_{mem} causes significant levels of heterotaxia. Thus, the normal pattern of V_{mem} is required for normal LR patterning. Consistent with this finding, it has already been shown that the normal asymmetric pattern of V_{mem} in chicks is required for normal LR asymmetry (Levin et al., 2002). Both pH and membrane voltage are important for downstream steps, and we are currently working to identify the mechanisms by which cellular ion fluxes are transduced to stable gene expression programs.

Disruption of consistent asymmetry by global manipulation of pH and/or V_{mem} suggests that the spatial distribution of the levels of these physiological parameters is important for asymmetry. How are the biophysical asymmetries in pH and/or V_{mem} coupled to downstream biochemical and genetic asymmetries? Active regulation of pH has been described during different stages of

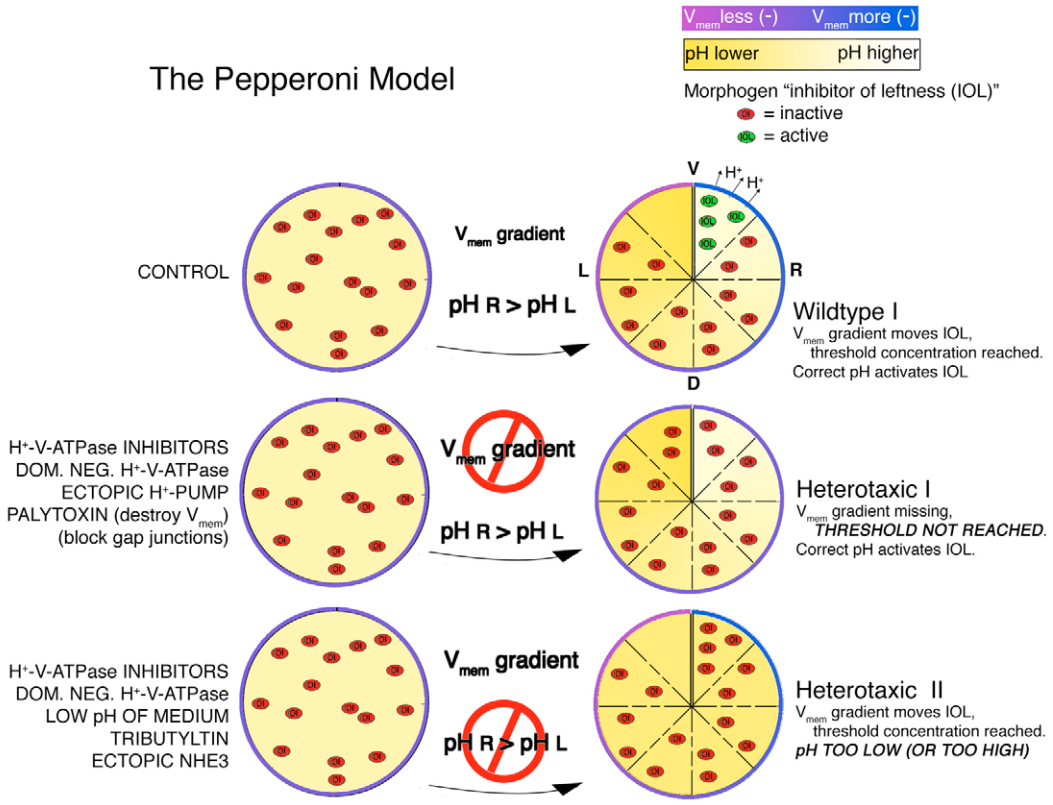

Fig. 9. Hypothesis for the role of H^+-V-ATPase in LR patterning; the pepperoni model. We propose the following model to account for the extant data on early LR patterning events in *Xenopus*. In control embryos, asymmetric H^+-V-ATPase activity is necessary for the establishment of both a pH and a V_{mem} gradient. The V_{mem} gradient provides the motive force to move a small charged morphogen (herein called 'inhibitor of leftness' or IOL) unidirectionally through gap junctions. Because there are no gap junctions connecting the two cells across the ventral midline (Levin and Mercola, 1998), the concentration of IOL will increase in the right ventral region. This increase in concentration is required for IOL activity, i.e. there is a threshold concentration for IOL to work. We further propose that IOL activity also requires a particular pH to function. Again, as a result of asymmetric H^+-V-ATPase activity, only the right ventral region reaches the required pH. Under these conditions, IOL can be active only in the right ventral region, where it triggers side-appropriate downstream events. Heterotaxia I: any treatment that interferes with the V_{mem} gradient will prevent IOL from reaching threshold concentration. We believe this explains the heterotaxia that results from treatments with H^+-V-ATPase inhibitors, expression of the dominant-negative subunit E, expression of ectopic H^+-pumps that change the normal pattern of H^+-flux and treatment with palytoxin, which destroys V_{mem} entirely. The concentration requirement also explains the heterotaxia caused by blocking GJC (Levin and Mercola, 1998), although the mechanism is distinct from that caused by changing V_{mem}. Heterotaxia II: This model also predicts that any treatment pushing the pH in the right ventral region beyond an acceptable range will cause heterotaxia. We believe this is why heterotaxia results when embryos are treated with H^+-V-ATPase inhibitors, dominant-negative subunit E, the low pH of the medium and the electroneutral change in pH caused by treatment with tributyltin or by expression of NHE3.

development (Gillespie and Greenwell, 1988; Grandin and Charbonneau, 1989). pH acts synergistically with many other important biochemical pathways (Busa and Nuccitelli, 1984), including Ca^{2+}-calmodulin binding and regulation of cAMP levels, which are important in LR patterning (Kawakami and Nakanishi, 2001). For example, pH gates gap junctions (Greenfield et al., 1990; Turin and Warner, 1980), which are essential for normal LR axis development (Levin and Mercola, 1999). pH regulation also has a role in gene expression and differentiation (Sater et al., 1994; Uzman et al., 1998) and in other important developmental processes such as proliferation, apoptosis and growth factor release (Bidani et al., 1998; Lee and Steinhardt, 1981; Putney and Barber, 2003; Shrode et al., 1997). pH also has other physiological effects that are likely to be important during development, although a direct connection has not been shown. For example, the G-protein-coupled receptors OGR1 and GPR4 are both inactive at pH 7.8. At pH 6.8, however, OGR1 leads to inositol phosphate formation, while GPR4 causes cAMP formation (Ludwig et al., 2003). Thus, pH changes can be coupled to two important second messengers. It is also known that certain ion channels are pH sensitive (Akopian et al., 2000; Berdiev et al., 2003), and H^+-V-ATPase could exert its effect by controlling another electrogenic component of LR patterning. There is also the possibility that activity of the asymmetrically localized H^+-V-ATPase could cause redistribution of determinants (which may include the H^+ ion itself) by virtue of electrophoretic forces driven by the strong voltage gradients that the H^+-V-ATPase can produce. One such plausible determinant is serotonin (5-HT). The normal localization of 5-HT to one blastomere at the 16-cell stage is required for asymmetry (Fukumoto et al., 2005b), and we observed that 5-HT cannot be detected by that stage in embryos exposed to H^+-V-ATPase inhibitors (Fig. 8D-G). One possibility, based on the requirement for vesicular monoamine transporters (VMAT) in asymmetry (Fukumoto et al., 2005a) and on the well-known role of the H^+-V-ATPase in powering 5-HT import into vesicles via the proton gradient-dependent transporter VMAT (Hayashi et al., 1999), is that 5-HT is degraded by monoamine oxidase when its import into protective vesicles is inhibited by downregulation of the H^+-V-ATPase. Thus, one likely link between H^+-V-ATPase function and downstream events is 5-HT signaling. However, the ability of asymmetry to be perturbed by cell-membrane modulation of pH and voltage suggests strongly that other linking mechanisms remain to be discovered. Although many of the downstream details remain to be worked out, we have formulated a model that accounts for the available data.

Hypothesis for the role of H^+ flux: the pepperoni model

We propose that a small charged morphogen, here hypothesized to be a positively charged inhibitor of left-side specific gene products (‘inhibitor of leftness’ or IOL), is evenly distributed in the fertilized egg, but becomes asymmetrically localized during early cleavage stages (Fig. 9). For this morphogen to be active, two requirements must be met: there must be a threshold concentration and there must be a high pH. The proposed V_{mem} gradient, established by the activity of the right-sided H^+-V-ATPase, and possibly the H^+/K^+-ATPase explored by Levin et al. (Levin et al., 2002), provides the unidirectional motive force that moves the morphogen, allowing the threshold concentration to be reached only on one side (the right). The asymmetric activity of the H^+-V-ATPase also raises the pH high enough to activate the morphogen, again, only on the right. Under these conditions the morphogen is active and affects the downstream genetic cascade only on the right side.

Because of the dual requirement for both threshold concentration and pH, manipulations that affect either of these conditions will cause heterotaxia. Heterotaxia I results when V_{mem} is disrupted. In that situation, although pH may be high enough to activate the morphogen, the threshold concentration has not been reached, and heterotaxia results. This may happen in embryos treated with H^+-V-ATPase inhibitors, expressing the electrogenic H^+-pump PMA1.2, or treated with the V_{mem} disrupting agent PTX. Heterotaxia II results when V_{mem} is normal, but pH is not high enough. Under those conditions, the threshold concentration may be reached, but pH is too low, and again, the morphogen remains inactive and heterotaxia results. This describes the situation in embryos treated with H^+-V-ATPase inhibitors, low pH medium or the electroneutral ionophore TBT, and in those embryos expressing the electroneutral NHE3. Testing this model and applying it to embryos of other species represents the next exciting challenge for future efforts to understand the integration of bioelectric and genetic information in left-right signaling.

We gratefully acknowledge the following for their contributions to this work: Debra Sorocco and Punita Koustubhan for animal and laboratory care; Shing-Ming Cheng for histology; and Dayong Qiu for molecular biology. For their kind gifts of reagents, we thank R. Shen for lobatomide analogs, M. Lu for YCHE78, C. Masuda and M. Montero-Lomeli for PMA1.2, R. Sabirov for NHE3, Y. Moriyama for anti-subunit A antibody, P. Backx for dominant negative Kir2.2, Kaethi Geering for the H,K-ATPase α subunit, W. Reith for anti-RFX3 antibody, M. Tosteson for palytoxin, and D. Stone and X. S. Xie for anti-A and anti-F subunit antibodies. We also thank Mark Mercola for important early discussions and the encouragement of this work at the beginning. This project was supported by NIH Training Grant 1-T32-DE-08327 and NIH Career Transition Award 1-K22-DE016633-01A1 to D.S.A; NSF grant IOB-0087517 to K.R.R; and NIH Research grant 1-R01-GM-0622, American Cancer Society Research Scholar Grant RSG-02-046-01-DDC and US Department of Transportation Grant to the FRCDB to M.L. This investigation was conducted in a Forsyth Institute facility renovated with support from Research Facilities Improvement Grant Number CO6RR11244 from the National Center for Research Resources, National Institutes of Health.

Supplementary material

Supplementary material for this article is available at
http://dev.biologists.org/cgi/content/full/133/9/1657/DC1

References

Adams, D. and Levin, M. (2006). Gap junctions and ion fluxes in patterning: strategies for investigating biophysical epigenetic control mechanisms in Xenopus. In *Analysis of Growth Factor Signaling in Embryos* (ed. M. Whitman and A. K. Sater). Boca Raton, FL: Taylor & Francis (in press).

Albertson, R. C. and Yelick, P. C. (2005). Roles for Fgf8 signaling in left-right patterning of the visceral organs and craniofacial skeleton. *Dev. Biol.* **283**, 310-321.

Akopian, A. N., Chen, C. C., Ding, Y., Cesare, P. and Wood, J. N. (2000). A new member of the acid-sensing ion channel family. *NeuroReport* **11**, 2217-2222.

Al-Awqati, Q. (1996). Plasticity in epithelial polarity of renal intercalated cells: targeting of the H(+)-ATPase and band 3. *Am. J. Physiol.* **270**, C1571-C1580.

Amack, J. D. and Yost, H. J. (2004). The T box transcription factor no tail in ciliated cells controls zebrafish left-right asymmetry. *Curr. Biol.* **14**, 685-690.

Arif, I., Newman, I. and Keenlyside, N. (1995). Proton flux measurements from tissues in buffered solutions. *Plant Cell Environ.* **18**, 1319-1324.

Ayscough, K. (1998). Use of latrunculin-A, an actin monomer-binding drug. *Meth. Enzymol.* **298**, 18-25.

Berdiev, B. K., Xia, J., McLean, L. A., Markert, J. M., Gillespie, G. Y., Mapstone, T. B., Naren, A. P., Jovov, B., Bubien, J. K., Ji, H. L. et al. (2003). Acid-sensing ion channels in malignant gliomas. *J. Biol. Chem.* **278**, 15023-15034.

Bidani, A., Wang, C. Z., Saggi, S. J. and Heming, T. A. (1998). Evidence for pH sensitivity of tumor necrosis factor-alpha release by alveolar macrophages. *Lung* **176**, 111-121.

Black, S. D. and Vincent, J. P. (1988). The first cleavage plane and the embryonic axis are determined by separate mechanisms in Xenopus laevis. II. Experimental dissociation by lateral compression of the egg. *Dev. Biol.* **128**, 65-71.

Bonnafe, E., Touka, M., AitLounis, A., Baas, D., Barras, E., Ucla, C., Moreau, A., Flamant, F., Dubruille, R., Couble, P. et al. (2004). The transcription factor RFX3 directs nodal cilium development and left-right asymmetry specification. *Mol. Cell. Biol.* **24**, 4417-4427.

Bowman, E. J., Siebers, A. and Altendorf, K. (1988). Bafilomycins: a class of inhibitors of membrane ATPases from microorganisms, animal cells, and plant cells. *Proc. Natl. Acad. Sci. USA* **85**, 7972-7976.
Brown, D. and Breton, S. (2000). H(+)V-ATPase-dependent luminal acidification in the kidney collecting duct and the epididymis/vas deferens: vesicle recycling and transcytotic pathways. *J. Exp. Biol.* **203**, 137-145.
Brown, D., Sabolic, I. and Gluck, S. (1992). Polarized targeting of V-ATPase in kidney epithelial cells. *J. Exp. Biol.* **172**, 231-243.
Brown, N. and Wolpert, L. (1990). The development of handedness in left/right asymmetry. *Development* **109**, 1-9.
Brown, N. A., Hoyle, C. I., McCarthy, A. and Wolpert, L. (1989). The development of asymmetry: the sidedness of drug-induced limb abnormalities is reversed in situs inversus mice. *Development* **107**, 637-642.
Buckler, K. J. and Vaughan-Jones, R. D. (1990). Application of a new pH-sensitive fluoroprobe (carboxy-SNARF-1) for intracellular pH measurement in small, isolated cells. *Pflugers Arch.* **417**, 234-239.
Bunney, T. D., De Boer, A. H. and Levin, M. (2003). Fusicoccin signaling reveals 14-3-3 protein function as a novel step in left-right patterning during amphibian embryogenesis. *Development* **130**, 4847-4858.
Burdine, R. and Schier, A. (2000). Conserved and divergent mechanisms in left-right axis formation. *Genes Dev.* **14**, 763-776.
Burn, J. (1991). Disturbance of morphological laterality in humans. *Ciba Found. Symp.* **162**, 282-296.
Busa, W. B. and Nuccitelli, R. (1984). Metabolic-regulation via intracellular Ph. *Am. J. Physiol.* **246**, R409-R438.
Chen, S. H., Bubb, M. R., Yarmola, E. G., Zuo, J., Jiang, J., Lee, B. S., Lu, M., Gluck, S. L., Hurst, I. R. and Holliday, L. S. (2004). Vacuolar H+-ATPase binding to microfilaments: regulation in response to phosphatidylinositol 3-kinase activity and detailed characterization of the actin-binding site in subunit B. *J. Biol. Chem.* **279**, 7988-7998.
Cooke, J. (2004). The evolutionary origins and significance of vertebrate left-right organisation. *BioEssays* **26**, 413-421.
Danilchik, M. V. and Black, S. D. (1988). The first cleavage plane and the embryonic axis are determined by separate mechanisms in Xenopus laevis. I. Independence in undisturbed embryos. *Dev. Biol.* **128**, 58-64.
Danos, M. C. and Yost, H. J. (1995). Linkage of cardiac left-right asymmetry and dorsal-anterior development in Xenopus. *Development* **121**, 1467-1474.
Danos, M. C. and Yost, H. J. (1996). Role of notochord in specification of cardiac left-right orientation in zebrafish and Xenopus. *Dev. Biol.* **177**, 96-103.
De Brabander, M., Geuens, G., Nuydens, R., Willebrords, R., Aerts, F. and De Mey, J. (1986). Microtubule dynamics during the cell cycle: the effects of taxol and nocodazole on the microtubule system of Pt K2 cells at different stages of the mitotic cycle. *Int. Rev. Cytol.* **101**, 215-274.
Drose, S., Bindseil, K. U., Bowman, E. J., Siebers, A., Zeeck, A. and Altendorf, K. (1993). Inhibitory effect of modified bafilomycins and concanamycins on P- and V-type adenosinetriphosphatases. *Biochemistry* **32**, 3902-3906.
Duboc, V., Rottinger, E., Lapraz, F., Besnardeau, L. and Lepage, T. (2005). Left-right asymmetry in the sea urchin embryo is regulated by nodal signaling on the right side. *Dev. Cell* **9**, 147-158.
Epps, D., Wolfe, M. and Groppi, V. (1994). Characterization of the steady-state and dynamic fluorescence properties of the potential-sensitive dye bis-(1,3-dibutylbarbituric acid)trimethine oxonol (Dibac4(3)) in model systems and cells. *Chem. Phys. Lipids* **69**, 137-150.
Essner, J., Vogan, K., Wagner, M., Tabin, C., Yost, H. and Brueckner, M. (2002). Conserved function for embryonic nodal cilia. *Nature* **418**, 37-38.
Essner, J. J., Amack, J. D., Nyholm, M. K., Harris, E. B. and Yost, H. J. (2005). Kupffer's vesicle is a ciliated organ of asymmetry in the zebrafish embryo that initiates left-right development of the brain, heart and gut. *Development* **133**, 1247-1260.
Finbow, M. E., John, S., Kam, E., Apps, D. K. and Pitts, J. D. (1993). Disposition and orientation of ductin (DCCD-reactive vacuolar H(+)-ATPase subunit) in mammalian membrane complexes. *Exp. Cell Res.* **207**, 261-270.
Fukumoto, T., Blakely, R. D. and Levin, M. (2005a). Serotonin transporter function is an early step in left-right patterning in chick and frog embryos. *Dev. Neurosci.* **27**, 349-363.
Fukumoto, T., Kema, I. P. and Levin, M. (2005b). Serotonin signaling is a very early step in patterning of the left-right axis in chick and frog embryos. *Curr. Biol.* **15**, 794-803.
Gillespie, J. I. and Greenwell, J. R. (1988). Changes in intracellular pH and pH regulating mechanisms in somitic cells of the early chick embryo: a study using fluorescent pH-sensitive dye. *J. Physiol.* **405**, 385-395.
Gluck, S. (1992). V-ATPases of the plasma membrane. *J. Exp. Biol.* **172**, 29-37.
Grandin, N. and Charbonneau, M. (1989). Intracellular pH and the increase in protein synthesis accompanying activation of Xenopus eggs. *Biol. Cell* **67**, 321-330.
Greenfield, L. J., Jr, Hackett, J. T. and Linden, J. (1990). Xenopus oocyte K+ current. III. Phorbol esters and pH regulate current at gap junctions. *Am. J. Physiol.* **259**, C792-C800.
Gross, S. P., Tuma, M. C., Deacon, S. W., Serpinskaya, A. S., Reilein, A. R. and Gelfand, V. I. (2002). Interactions and regulation of molecular motors in Xenopus melanophores. *J. Cell Biol.* **156**, 855-865.
Hamada, H., Meno, C., Watanabe, D. and Saijoh, Y. (2002). Establishment of vertebrate left-right asymmetry. *Nat. Rev. Genet.* **3**, 103-113.
Hamburger, V. and Hamilton, H. (1992). A series of normal stages in the development of the chick embryo. *Dev. Dyn.* **195**, 231-272.
Harland, R. M. (1991). In situ hybridization: an improved whole mount method for *Xenopus* embryos. In *Xenopus laevis: Practical uses in Cell and Molecular Biology*, *vol. 36* (ed. B. K. Kay and H. B. Peng), pp. 685-695. San Diego: Academic Press.
Harvey, R. P. and Melton, D. A. (1988). Microinjection of synthetic Xhox-1A homeobox mRNA disrupts somite formation in developing Xenopus embryos. *Cell* **53**, 687-697.
Harvey, W. (1992). Physiology of V-ATPases. In *V-ATPases*, Vol. 172 (ed. W. Harvey and N. Nelson), pp. 1-17. Philadelphia, PA: Temple University.
Harvey, W. R. and Wieczorek, H. (1997). Animal plasma membrane energization by chemiosmotic H+ V-ATPases. *J. Exp. Biol.* **200**, 203-216.
Hayashi, M., Haga, M., Yatsushiro, S., Yamamoto, A. and Moriyama, Y. (1999). Vesicular monoamine transporter 1 is responsible for storage of 5-hydroxytryptamine in rat pinealocytes. *J. Neurochem.* **73**, 2538-2545.
Hibino, T., Yuichiro, I., Levin, M. and Nishino, A. (2006). Ion flow regulates left-right asymmetry in sea urchin development. *Dev. Genes Evol.* (in press).
Hilgemann, D. W. (2003). From a pump to a pore: how palytoxin opens the gates. *Proc. Natl. Acad. Sci. USA* **100**, 386-388.
Hotary, K. B., Nuccitelli, R. and Robinson, K. R. (1992). A computerized 2-dimensional vibrating probe for mapping extracellular current patterns. *J. Neurosci. Meth.* **43**, 55-67.
Huss, M., Ingenhorst, G., Konig, S., Gassel, M., Drose, S., Zeeck, A., Altendorf, K. and Wieczorek, H. (2002). Concanamycin A, the specific inhibitor of V-ATPases, binds to the Vo subunit c. *J. Biol. Chem.* **277**, 40544-40548.
Hyatt, B. A., Lohr, J. L. and Yost, H. J. (1996). Initiation of vertebrate left-right axis formation by maternal Vg1. *Nature* **384**, 62-65.
Inoue, T., Wilkens, S. and Forgac, M. (2003). Subunit structure, function, and arrangement in the yeast and coated vesicle V-ATPases. *J. Bioenerg. Biomembr.* **35**, 291-299.
Kawa, G., Yamamoto, A., Yoshimori, T., Muguruma, K., Matsuda, T. and Moriyama, Y. (2000). Immunohistochemical localization of V-ATPases in rat spermatids. *Int. J. Androl.* **23**, 278-283.
Kawakami, M. and Nakanishi, N. (2001). The role of an endogenous PKA inhibitor, PKIalpha, in organizing left-right axis formation. *Development* **128**, 2509-2515.
Kawakami, Y., Raya, A., Raya, R. M., Rodriguez-Esteban, C. and Belmonte, J. C. (2005). Retinoic acid signalling links left-right asymmetric patterning and bilaterally symmetric somitogenesis in the zebrafish embryo. *Nature* **435**, 165-171.
Kawasaki-Nishi, S., Nishi, T. and Forgac, M. (2003). Proton translocation driven by ATP hydrolysis in V-ATPases. *FEBS Lett.* **545**, 76-85.
Klein, S. L. (1987). The first cleavage furrow demarcates the dorsal-ventral axis in Xenopus embryos. *Dev. Biol.* **120**, 299-304.
Klein, U., Timme, M., Zeiske, W. and Ehrenfeld, J. (1997). The H+ pump in frog skin (Rana esculenta): identification and localization of a V-ATPase. *J. Membr. Biol.* **157**, 117-126.
Kosaki, K. and Casey, B. (1998). Genetics of human left-right axis malformations. *Semin. Cell Dev. Biol.* **9**, 89-99.
Kramer, K. L., Barnette, J. E. and Yost, H. J. (2002). PKCgamma regulates syndecan-2 inside-out signaling during xenopus left-right development. *Cell* **111**, 981-990.
Kramer-Zucker, A. G., Olale, F., Haycraft, C. J., Yoder, B. K., Schier, A. F. and Drummond, I. A. (2005). Cilia-driven fluid flow in the zebrafish pronephros, brain and Kupffer's vesicle is required for normal organogenesis. *Development* **132**, 1907-1921.
Lee, B. S., Gluck, S. L. and Holliday, L. S. (1999). Interaction between vacuolar H(+)-ATPase and microfilaments during osteoclast activation. *J. Biol. Chem.* **274**, 29164-29171.
Lee, S. C. and Steinhardt, R. A. (1981). Observations on intracellular pH during cleavage of eggs of Xenopus laevis. *J. Cell Biol.* **91**, 414-419.
Levin, M. (1999). Twinning and embryonic left-right asymmetry. *Laterality* **4**, 197-208.
Levin, M. (2003a). Bioelectromagnetic patterning fields: roles in embryonic development, regeneration, and neoplasm. *Bioelectromagnetics* **24**, 295-315.
Levin, M. (2003b). Electric embryos: endogenous ion fluxes and voltage gradients in left-right asymmetry. *Dev. Biol.* **259**, 482.
Levin, M. (2003c). Hypothesis: motor proteins and ion pumps, not ciliary motion, initiate LR asymmetry. *BioEssays* **25**, 1002-1010.
Levin, M. (2004). A novel immunohistochemical method for evaluation of antibody specificity and detection of labile targets in biological tissue. *J. Biochem. Biophys. Meth.* **58**, 85-96.

Levin, M. (2005). Left-right asymmetry in embryonic development: a comprehensive review. *Mech. Dev.* **122**, 3-25.
Levin, M. and Mercola, M. (1998). Gap junctions are involved in the early generation of left right asymmetry. *Dev. Biol.* **203**, 90-105.
Levin, M. and Mercola, M. (1999). Gap junction-mediated transfer of left-right patterning signals in the early chick blastoderm is upstream of Shh asymmetry in the node. *Development* **126**, 4703-4714.
Levin, M., Johnson, R., Stern, C., Kuehn, M. and Tabin, C. (1995). A molecular pathway determining left-right asymmetry in chick embryogenesis. *Cell* **82**, 803-814.
Levin, M., Roberts, D., Holmes, L. and Tabin, C. (1996). Laterality defects in conjoined twins. *Nature* **384**, 321.
Levin, M., Thorlin, T., Robinson, K. R., Nogi, T. and Mercola, M. (2002). Asymmetries in H+/K+-ATPase and cell membrane potentials comprise a very early step in left-right patterning. *Cell* **111**, 77-89.
Lohr, J. L., Danos, M. C., Groth, T. W. and Yost, H. J. (1998). Maintenance of asymmetric nodal expression in Xenopus laevis. *Dev. Genet.* **23**, 194-202.
Long, S., Ahmad, N. and Rebagliati, M. (2003). The zebrafish nodal-related gene southpaw is required for visceral and diencephalic left-right asymmetry. *Development* **130**, 2303-2316.
Lowe, L., Supp, D., Sampath, K., Yokoyama, T., Wright, C., Potter, S., Overbeek, P. and Kuehn, M. (1996a). Conserved left-right asymmetry of nodal expression and alterations in murine situs inversus. *Nature* **381**, 158-161.
Lowe, L. A., Supp, D. M., Sampath, K., Yokoyama, T., Wright, C. V., Potter, S. S., Overbeek, P. and Kuehn, M. R. (1996b). Conserved left-right asymmetry of nodal expression and alterations in murine situs inversus. *Nature* **381**, 158-161.
Lu, M., Vergara, S., Zhang, L., Holliday, L. S., Aris, J. and Gluck, S. L. (2002). The amino-terminal domain of the E subunit of vacuolar H(+)-ATPase (V-ATPase) interacts with the H subunit and is required for V-ATPase function. *J. Biol. Chem.* **277**, 38409-38415.
Ludwig, M. G., Vanek, M., Guerini, D., Gasser, J. A., Jones, C. E., Junker, U., Hofstetter, H., Wolf, R. M. and Seuwen, K. (2003). Proton-sensing G-protein-coupled receptors. *Nature* **425**, 93-98.
Masho, R. (1990). Close correlation between the 1st cleavage plane and the body axis in early Xenopus embryos. *Dev. Growth Differ.* **32**, 57-64.
Masuda, C. A. and Montero-Lomeli, M. (2000). An NH2-terminal deleted plasma membrane H+-ATPase is a dominant negative mutant and is sequestered in endoplasmic reticulum derived structures. *Biochem. Cell Biol.* **78**, 51-58.
Mathews, P. M., Claeys, D., Jaisser, F., Geering, K., Horisberger, J. D., Kraehenbuhl, J. P. and Rossier, B. C. (1995). Primary structure and functional expression of the mouse and frog alpha-subunit of the gastric H(+)-K(+)-ATPase. *Am. J. Physiol.* **268**, C1207-C1214.
Matsuya, H., Okamoto, M., Ochi, T., Nishikawa, A., Shimizu, S., Kataoka, T., Nagai, K., Wasserman, H. H. and Ohkuma, S. (2000). Reversible and potent uncoupling of hog gastric (H(+)+K(+))-ATPase by prodigiosins. *Biochem. Pharmacol.* **60**, 1855-1863.
McGrath, J. and Brueckner, M. (2003). Cilia are at the heart of vertebrate left-right asymmetry. *Curr. Opin. Genet. Dev.* **13**, 385-392.
McGrath, J., Somlo, S., Makova, S., Tian, X. and Brueckner, M. (2003). Two populations of node monocilia initiate left-right asymmetry in the mouse. *Cell* **114**, 61-73.
Mitchison, T. J. (1994). Towards a pharmacological genetics. *Chem. Biol.* **1**, 3-6.
Morley, G. E., Taffet, S. M. and Delmar, M. (1996). Intramolecular interactions mediate pH regulation of connexin43 channels. *Biophys. J.* **70**, 1294-1302.
Narbaitz, R., Bastani, B., Galvin, N. J., Kapal, V. K. and Levine, D. Z. (1995). Ultrastructural and immunocytochemical evidence for the presence of polarised plasma membrane H(+)-ATPase in two specialised cell types in the chick embryo chorioallantoic membrane. *J. Anat.* **186**, 245-252.
Nieuwkoop, P. D. and Faber, J. (1967). Normal Table of *Xenopus laevis* (Daudin). Amsterdam: North-Holland Publishing Company.
Nishi, T. (2002). The vacuolar (H+)-ATPases – nature's most versatile proton pumps. *Nat. Rev. Mol. Cell Biol.* **3**, 94-103.
Nonaka, S., Tanaka, Y., Okada, Y., Takeda, S., Harada, A., Kanai, Y., Kido, M. and Hirokawa, N. (1998). Randomization of left-right asymmetry due to loss of nodal cilia generating leftward flow of extraembryonic fluid in mice lacking KIF3B motor protein. *Cell* **95**, 829-837.
Nuccitelli, R. (2003). Endogenous electric fields in embryos during development, regeneration and wound healing. *Radiat. Prot. Dosimetry* **106**, 375-383.
Okada, Y., Takeda, S., Tanaka, Y., Belmonte, J. C. and Hirokawa, N. (2005). Mechanism of nodal flow: a conserved symmetry breaking event in left-right axis determination. *Cell* **121**, 633-644.
Payne-Ferreira, T. L. and Yelick, P. C. (2003). Alk8 is required for neural crest cell formation and development of pharyngeal arch cartilages. *Dev. Dyn.* **228**, 683-696.
Peng, S. B., Crider, B. P., Tsai, S. J., Xie, X. S. and Stone, D. K. (1996). Identification of a 14-kDa subunit associated with the catalytic sector of clathrin-coated vesicle H+-ATPase. *J. Biol. Chem.* **271**, 3324-3327.
Praetorius, J., Andreasen, D., Jensen, B. L., Ainsworth, M. A., Friis, U. G. and Johansen, T. (2000). NHE1, NHE2, and NHE3 contribute to regulation of intracellular pH in murine duodenal epithelial cells. *Am. J. Physiol. Gastrointest. Liver Physiol.* **278**, G197-G206.
Putney, L. K. and Barber, D. L. (2003). Na-H exchange-dependent increase in intracellular pH times G2/M entry and transition. *J. Biol. Chem.* **278**, 44645-44649.
Qiu, D., Cheng, S. M., Wozniak, L., McSweeney, M., Perrone, E. and Levin, M. (2005). Localization and loss-of-function suggest early, cytoplasmic roles for 'ciliary' proteins in embryonic left-right asymmetry. *Dev. Dyn.* **234**, 176-189.
Raya, A. and Belmonte, J. C. (2004). Sequential transfer of left-right information during vertebrate embryo development. *Curr. Opin. Genet. Dev.* **14**, 575-581.
Raya, A., Kawakami, Y., Rodriguez-Esteban, C., Ibanes, M., Rasskin-Gutman, D., Rodriguez-Leon, J., Buscher, D., Feijo, J. A. and Izpisua Belmonte, J. C. (2004). Notch activity acts as a sensor for extracellular calcium during vertebrate left-right determination. *Nature* **427**, 121-128.
Sabirov, R. Z., Azimov, R. R., Ando-Akatsuka, Y., Miyoshi, T. and Okada, Y. (1999). Na(+) sensitivity of ROMK1 K(+) channel: role of the Na(+)/H(+) antiporter. *J. Membr. Biol.* **172**, 67-76.
Sater, A. K., Alderton, J. M. and Steinhardt, R. A. (1994). An increase in intracellular pH during neural induction in Xenopus. *Development* **120**, 433-442.
Scarborough, G. A. (2000). The plasma membrane proton-translocating ATPase. *Cell. Mol. Life Sci.* **57**, 871-883.
Shen, R., Lin, C. T., Bowman, E. J., Bowman, B. J. and Porco, J. A., Jr (2002). Synthesis and V-ATPase inhibition of simplified lobatamide analogues. *Org. Lett.* **4**, 3103-3106.
Shen, R., Lin, C. T., Bowman, E. J., Bowman, B. J. and Porco, J. A., Jr (2003). Lobatamide C: total synthesis, stereochemical assignment, preparation of simplified analogues, and V-ATPase inhibition studies. *J. Am. Chem. Soc.* **125**, 7889-7901.
Shimeld, S. M. and Levin, M. (2006). Evidence for the regulation of left-right asymmetry in *Ciona intestinalis* by ion flux. *Dev. Dyn.* (in press).
Shrode, L. D., Tapper, H. and Grinstein, S. (1997). Role of intracellular pH in proliferation, transformation, and apoptosis. *J. Bioenerg. Biomembr.* **29**, 393-399.
Simchowitz, L., Textor, J. A. and Vogt, S. K. (1991). Use of tributyltin to probe contribution of Cl(–)-HCO_3^- exchange to regulation of steady-state pHi in human neutrophils. *Am. J. Physiol.* **261**, C906-C915.
Sive, H., Grainger, R. M. and Harland, R. (2000). *Early Development of* Xenopus laevis. Cold Spring Harbor, New York: Cold Spring Harbor Laboratory Press.
Smith, P. J. and Trimarchi, J. (2001). Noninvasive measurement of hydrogen and potassium ion flux from single cells and epithelial structures. *Am. J. Physiol. Cell Physiol.* **280**, C1-C11.
Smith, P. J., Hammar, K., Porterfield, D. M., Sanger, R. H. and Trimarchi, J. R. (1999). Self-referencing, non-invasive, ion selective electrode for single cell detection of trans-plasma membrane calcium flux. *Microsc. Res. Tech.* **46**, 398-417.
Stern, C. and Holland, P. (1993). *Essential Developmental Biology: A Practical Approach*. Oxford: IRL Press at Oxford University Press.
Sun-Wada, G., Murata, Y., Yamamoto, A., Kanazawa, H., Wada, Y. and Futai, M. (2000). Acidic endomembrane organelles are required for mouse postimplantation development. *Dev. Biol.* **228**, 315-325.
Supp, D. M., Witte, D. P., Potter, S. S. and Brueckner, M. (1997). Mutation of an axonemal dynein affects left-right asymmetry in inversus viscerum mice. *Nature* **389**, 963-966.
Tabin, C. J. and Vogan, K. J. (2003). A two-cilia model for vertebrate left-right axis specification. *Genes Dev.* **17**, 1-6.
Tanaka, Y., Okada, Y. and Hirokawa, N. (2005). FGF-induced vesicular release of Sonic hedgehog and retinoic acid in leftward nodal flow is critical for left-right determination. *Nature* **435**, 172-177.
Tosteson, M. T., Scriven, D. R., Bharadwaj, A., Arnadottir, J. and Tosteson, D. C. (1997). Interactions of palytoxin with the Na,K-ATPase. Where are those sites? *Ann. N. Y. Acad. Sci.* **834**, 424-425.
Tosteson, M. T., Thomas, J., Arnadottir, J. and Tosteson, D. C. (2003). Effects of palytoxin on cation occlusion and phosphorylation of the (Na+,K+)-ATPase. *J. Membr. Biol.* **192**, 181-189.
Turin, L. and Warner, A. E. (1980). Intracellular pH in early Xenopus embryos: its effect on current flow between blastomeres. *J. Physiol.* **300**, 489-504.
Uzman, J. A., Patil, S., Uzgare, A. R. and Sater, A. K. (1998). The role of intracellular alkalinization in the establishment of anterior neural fate in Xenopus. *Dev. Biol.* **193**, 10-20.
Vitavska, O., Wieczorek, H. and Merzendorfer, H. (2003). A novel role for subunit C in mediating binding of the H(+)-V-ATPase to the actin cytoskeleton. *J. Biol. Chem.* **278**, 18499-18505.
Vize, P. D., Melton, D. A., Hemmati-Brivanlou, A. and Harland, R. M. (1991). Assays for gene function in developing Xenopus embryos. *Meth. Cell Biol.* **36**, 367-387.

Warner, A. E., Guthrie, S. C. and Gilula, N. B. (1984). Antibodies to gap-junctional protein selectively disrupt junctional communication in the early amphibian embryo. *Nature* **311**, 127-131.
Westerfield, M. (1995). *The Zebrafish Book*. Eugene, OR: University of Oregon Press.
Wheatly, M. G. and Gao, Y. (2004). Molecular biology of ion motive proteins in comparative models. *J. Exp. Biol.* **207**, 3253-3263.
Whitman, M. and Mercola, M. (2001). TGF-beta superfamily signaling and left-right asymmetry. *Sci. STKE* 2001, RE1.
Wieczorek, H. (1999). Animal plasma membrane energization by proton-motive V-ATPases. *BioEssays* **21**, 637-648.
Woo, J., Ohba, Y., Tagami, K., Sumitani, K., Yamaguchi, K. and Tsuji, T. (1996). Concanamycin B, a vacuolar H(+)-ATPase specific inhibitor suppresses bone resorption in vitro. *Biol. Pharm. Bull.* **19**, 297-299.
Yost, H. J. (1991). Development of the left-right axis in amphibians. *Ciba Found. Symp.* **162**, 165-176.
Yost, H. J. (2001). Establishment of left-right asymmetry. *Int. Rev. Cytol.* **203**, 357-381.
Zobel, C., Cho, H. C., Nguyen, T. T., Pekhletski, R., Diaz, R. J., Wilson, G. J. and Backx, P. H. (2003). Molecular dissection of the inward rectifier potassium current (IK1) in rabbit cardiomyocytes: evidence for heteromeric co-assembly of Kir2.1 and Kir2.2. *J. Physiol.* **550**, 365-372.